ARO 14585.1-E

LEVEL II

EFFECT OF STRUCTURAL PARAMETERS ON

THE FLAP-LAG RESPONSE OF A ROTOR

BLADE IN FORWARD FLIGHT

Interim Technical Report No. 1

by
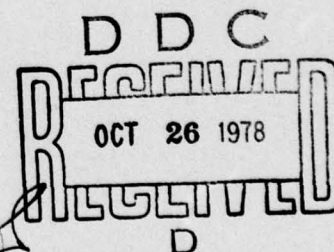
David A. Peters

and

Daniel P. Schrage

July 1978

Washington University

School of Engineering and Applied Science

St. Louis, Missouri 63130

D D C

RECEIVED

OCT 26 1978

D

78 10 19 025

LEVEL II

⑥ EFFECT OF STRUCTURAL PARAMETERS ON
THE FLAP-LAG RESPONSE OF A ROTOR
BLADE IN FORWARD FLIGHT.

⑨ Interim Technical Report No. 1, Mar. 77-Jun 78,

by

⑩ David A. / Peters
~~and~~
Daniel P. / Schrage

⑪ July 1978

⑫ 107p.

U.S. Army Research Office
Grant No. ⑮ DAAG29-77-G-0103

Washington University   Dept of mechanical Engineering
School of Engineering and Applied Science
St. Louis, Missouri 63130

⑱ ARO   ⑲ 14585.1-E

Approved for public release;
distribution unlimited.

D D C
RECEIVED
OCT 26 1978
D

New
410901

REPORT DOCUMENTATION PAGE		READ INSTRUCTIONS BEFORE COMPLETING FORM
1. REPORT NUMBER 1	2. GOVT ACCESSION NO.	3. RECIPIENT'S CATALOG NUMBER
4. TITLE (and Subtitle) Effect of Structural Parameters on the Flap-Lag Response of a Rotor Blade in Forward Flight		5. TYPE OF REPORT & PERIOD COVERED Interim Technical March 1977-June 1978
		6. PERFORMING ORG. REPORT NUMBER
7. AUTHOR(s) David A. Peters and Daniel P. Schrage		8. CONTRACT OR GRANT NUMBER(s) DAAG29-77-G-0103 ew
9. PERFORMING ORGANIZATION NAME AND ADDRESS Department of Mechanical Engineering Washington University, Box 1185 St. Louis, MO 63130		10. PROGRAM ELEMENT, PROJECT, TASK AREA & WORK UNIT NUMBERS NA
11. CONTROLLING OFFICE NAME AND ADDRESS U. S. Army Research Office Post Office Box 12211 Research Triangle Park, NC 27709		12. REPORT DATE July 1978
		13. NUMBER OF PAGES 104
14. MONITORING AGENCY NAME & ADDRESS(if different from Controlling Office) Office of Naval Research Branch Office Chicago 536 South Clark Street Chicago, IL 60605		15. SECURITY CLASS. (of this report) Unclassified
		15a. DECLASSIFICATION/DOWNGRADING SCHEDULE NA

16. DISTRIBUTION STATEMENT (of this Report)

Approved for public release; distribution unlimited.

17. DISTRIBUTION STATEMENT (of the abstract entered in Block 20, if different from Report)

NA

18. SUPPLEMENTARY NOTES

The findings in this report are not to be construed as an official Department of the Army position, unless so designated by other authorized documents.

19. KEY WORDS (Continue on reverse side if necessary and identify by block number)

Helicopter, Response, Rotor

20. ABSTRACT (Continue on reverse side if necessary and identify by block number)

See page i

DD FORM 1473 (1 JAN 73)   EDITION OF 1 NOV 65 IS OBSOLETE

The findings of this report are not to be construed as an official Department of the Army position, unless so designated by other authorized documents.

EFFECT OF STRUCTRUAL PARAMETERS ON THE FLAP-LAG RESPONSE OF A ROTOR BLADE IN FORWARD FLIGHT

Abstract

This interim report covers a completed portion of the research on this grant. In this portion of the research, a study is made of the effect of structural coupling on the vibrations of rigid, centrally hinged rotor blades. In particular, the research is aimed at discovering if the parameter combinations that result in desirable stability characteristics might also result in good vibrational characteristics. In order to determine the stability and vibrations simultaneously, a new analytical method, based on eigenvalue and modal decoupling, is developed to solve for the eigenvalues and forced response of systems of equations with periodic coefficients. This method is then applied to the linearized equations of motion for rotor flap-lag in forward flight. Unlike conventional linear analyses, however, this analysis retains the nonlinear terms as added forcing functions.

The eigenvalue and modal decoupling method and equations of motion are then applied to four realistic rotor configurations: an articulated main rotor with lag damper, a soft inplane main rotor, and two stiff inplane tail rotors. The vibrations of each rotor are calculated for a baseline configuration and compared with experimental data for similar rotors whenever possible. Then each of the major coupling parameters is varied in order to determine its influence on stability and vibrations. The results

show that the major coupling parameters can be rationally chosen so as to give both good stability and good vibrations. Elastic coupling can be chosen to reduce inplane loads, pitch-flap-coupling can be chosen to reduce flapping loads, and pitch-lag coupling can be chosen to increase blade damping.

iii

TABLE OF CONTENTS

TABLE OF CONTENTS
(continued)

v

LIST OF TABLES

LIST OF FIGURES

LIST OF FIGURES
(continued)

EFFECT OF STRUCTURAL PARAMETERS ON THE FLAP-LAG FORCED

RESPONSE OF A ROTOR BLADE IN FORWARD FLIGHT

1. INTRODUCTION

1.1 STATEMENT OF THE PROBLEM

Compared to the conventional airplane, the present day
helicopter is a modern invention. Although Leonardo da Vinci
sketched a man-carrying vehicle with rotating wings around
the year 1500, only after World War II has this versatile
aircraft come into general use throughout the world. During
the last decade the helicopter has become one of man's most
useful tools in the air, demonstrating its versatility in
both civil and military roles. The reasons for the long
delay in realizing Leonardo's dream have not been for want
of trying.

If we consider the first flight of de la Cierva's
autogyros in 1925-26 as the birth of rotary-wing aviation,
then the "childhood diseases" of the helicopter were mainly
solved in the first decade (1926-1936). These initial
problems were aerodynamic in nature and consisted of balanc-
ing, controllability and stability. More serious deficiencies
became apparent, however, when the first series-produced

machines appeared and were placed in service. These problems were dynamic in nature such as fatigue due to insufficient dynamic strength of certain structural members and degradation of crew and passenger efficiency due to unacceptable vibration levels (1)*. While sufficient control of these deficiencies has been achieved to allow the helicopter to progress to its present state, they remain as a major obstacle in complete maturity phase development of the helicopter.

The loads on the helicopter are quite different from those of a conventional propeller driven aircraft. The propeller operates practically in an axial flow and, like an engine, sets up no noticeable variable stresses in the structural members. Therefore, it is only during take-off, landing, and maneuvers that appreciable dynamic loads are induced on the aircraft structure. Since these loads usually represent relatively few load cycles during the lifetime of the aircraft, one can generally speak of repeated static loads. The helicopter's main structural members are loaded dynamically, the number of loadings often exceeding tens of millions of cycles during its lifetime. The cause of this dynamic loading is due primarily to the asymmetric airflow past the main rotor as it rotates and simultaneously advances (1).

---

* The numbers in parentheses in the text indicate references in the Bibliography.

In forward flight, when the main rotor provides both lift and propulsive force for the helicopter, the flow over the blades is asymmetric due to the velocity differential over the advancing and retreating blades (Figure 1). Rotor control is obtained by "cyclic pitch" change, which is the name given to the first harmonic variation applied to the blade pitch angle as it rotates. Since the relative air velocity over the blade also has a first harmonic variation and since aerodynamic forces are proportional to the square of the relative velocity, we may expect to find at least three harmonics in the force fluctuations acting on the blades. This would be true if the airflow through the rotor were uniform. However, due to the proximity of the rotor to its own vortex wake, which is swept backwards under the rotor disc, the flow is far from uniform; and velocity fluctuations are induced which give rise to very many harmonics of blade loading. The aerodynamic characteristics of a rotor in forward flight give rise to shear forces and moments at the blade root which are then transmitted to the rotor hub where they are combined and sent through the rotor shaft into the airframe.

During the design of a helicopter, accurate prediction of main rotor blade and hub oscillatory loading is important for fatigue, vibration, and forward flight performance. Critical dynamic components are designed for fatigue based on these predicted loads. Vibration characteristics of the
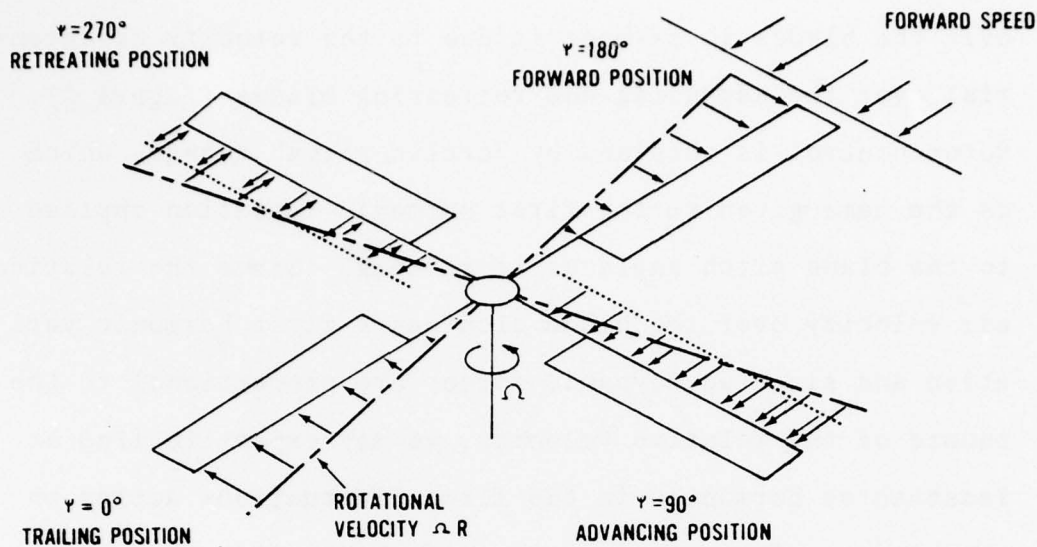
Figure 1.   Rotor Blade Azimuths and Velocities

airframe and the need for vibration-reduction devices are
determined from these loads. Since vibratory response and
rotor loads usually determine limiting speed and load-factor
operational envelopes, the predicted loads greatly influence
forward flight performance. Recent Army helicopter develop-
ment programs, Utility Tactical Transport Aircraft System
(UTTAS) and Advanced Attack Helicopter (AAH), have revealed
that these loads cannot be predicted accurately (2). A
similar conclusion was drawn from a comparison study(3)
where the helicopter industry's major state-of-the-art rotor
loads analyses were independently exercised on an identical
hypothetical helicopter problem. The comparison of results

illustrated significant differences, particularly in structural dynamic modeling, between the various analyses. A strong recommendation as a result of this study was to conduct computer experiments to study specific isolated aspects of the solution methods and structural dynamics (3). It was the results of this study and the UTTAS/AAH Programs that provided the impetus for this research.

1.2 PREVIOUS WORK

It has been stated that the prediction of rotor blade vibrations is one of the most difficult analytical problems in rotary wing technology since it involves a highly non-linear aeroelastic response problem. Elements necessary for a complete analysis are illustrated in the block diagram of Figure 2. The approach taken by industry has been to develop
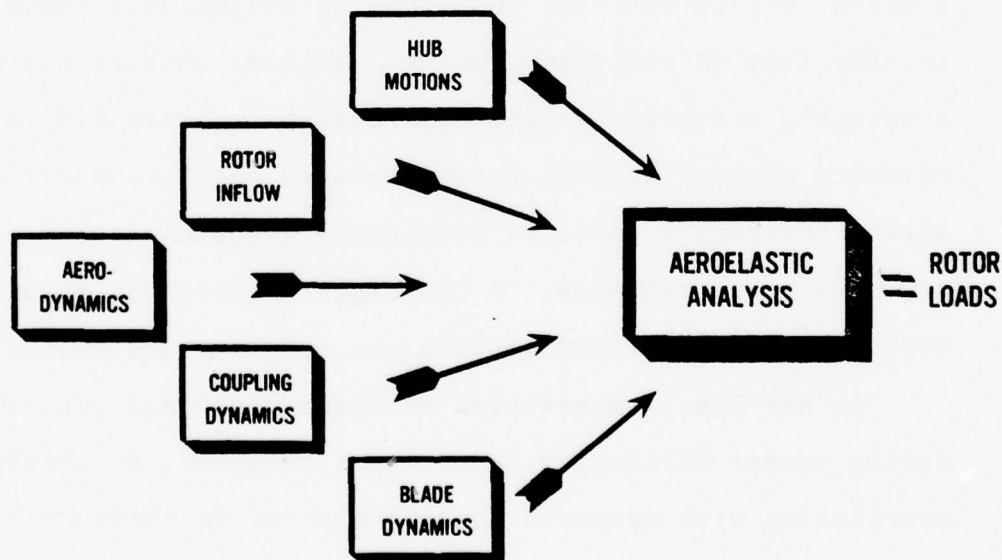
Figure 2. Rotor Loads Analysis

large mathematical models to incorporate as many necessary
elements as possible. A general description of several of
these models are described in Reference 3-6.

The various methods can be classified according to the
form of the equations (modal or finite element) and the
method of solution (harmonic balance or numerical inte-
gration). The modal equations are obtained from the partial
differential equations of a rotating beam with the general-
ized coordinates of the normal modes as the system degrees
of freedom. Finite element equations are based on the force
and moment equilibrium of lumped segments of the blade.
Therefore, each element requires several degrees of freedom.
Both of these methods require coupling between the various
degrees of freedom. Solution methods using numerical inte-
gration require that the equations of motion be integrated
in time from an arbitrary, assumed initial condition until
a suitably converged solution is obtained. Harmonic response
solution methods usually calculate structural response using
airload harmonics based on previously assumed blade motion
and structural response. A converged solution is obtained
through many iterations between the response and airload (3).

As has been demonstrated in Reference 3 and verified
during recent helicopter development programs, to obtain
correlation with measured loads the input to these programs
must be adjusted empirically utilizing experimental data.
These results emphasized that there is a lack of fundamental
understanding of the structural dynamics that participate in

creating blade vibrations. Reference 3 also showed that there is no consensus on the best method to use in the computation of the trim solution from which vibrational data is obtained. There is presently no way to predict the numerical stability of the calculation methods. This need for fundamental research has been recognized by industry (7), as well as government (2,3).

While some attempts have been made to utilize existing large computer programs in this type of fundamental research (5,8) much can be learned on a more basic level by studies using greatly simplified mathematical models. The large programs are very complex and expensive to run. The voluminous amount of input required often obscures the importance of certain parameters. Unfortunately, few simplified procedures give meaningful results.

1.3 SCOPE OF WORK

The objective of this research is to extend a method developed to study rotor stability to include the calculation of forced response. A simplified model has been used, but one that includes the effects of pitch-flap and pitch-lag structural coupling, flap-lag elastic coupling and a blade lag damper. The combined forced response and stability method is an eigenvalue and modal decoupling analysis.

The procedure followed is to derive the flap-lag equations of motion for a helicopter blade in forward flight. Perturbation theory is applied to obtain linear free vibration equations, although the appropriate nonlinear terms are

retained on the right-hand side of the system equations as forcing functions. Numerical methods are used to solve the equations by the eigenvalue and modal decoupling method in order to obtain the flap and lag responses. These responses are then utilized to obtain the shears and moments at the rotor hub in the rotating and nonrotating systems. A base-line case from Reference 3 is used to verify the model and the method. Other rotor configurations are then used to study the effects of structural parameters on both the flap-lag forced response and the stability of a helicopter rotor blade in forward flight.

2. MATHEMATICAL BACKGROUND

The eigenvalue and modal decoupling analysis that has been used to study the flap-lag forced response and stability of a helicopter rotor blade in forward flight is based on several mathematical methods.

2.1 STATE VARIABLE THEORY

As was stated in the Introduction, the flap-lag equations of motion for a helicopter rotor in forward flight are non-linear differential equations with periodic coefficients. These equations can be linearized by considering small per-turbation motions about a periodic equilibrium motion of the nonlinear system. For the rotor blade, this periodic equilib-rium motion is a periodic trimmed solution where the rotor blades forces and moments are in equilibrium. It is useful to write the equations (for perturbations about this equilibrium) in state variable form. A state variable in a system of differential equations can be either any variable whose output appears at an integrator or any one-to-one function of these variables (9). A more qualitative descrip-tion might be that a state is any internal characteristic of a system that somehow summarizes at each time those properties of the past input history that are pertinent to the deter-mination of the present output and, along with the future inputs, the determination of future outputs. For many dynamical systems the state vector is composed of the veloc-ity and displacement of each degree of freedom of the system.

This allows a system of second order differential equations to be written as a system of first order differential equations:

$$\{\dot{x}(t)\} + [D(t)]\{x(t)\} = \{f(t)\} \qquad (2.1)$$

where $\{x(t)\} = \begin{Bmatrix} \dot{y} \\ y \end{Bmatrix}$, the state vector

Most computer library differential equation solvers require the equations be written in state form.

The solutions for a system of differential equations with periodic coefficients are closely associated with the concept of the state transition matrix, which is a matrix whose columns contain the linearly independent solutions to the above system of equations. In general, this matrix can be written as:

$$\phi(t,t_o) = \Big[\phi_1(t,t_o), \phi_2(t,t_o), \phi_3(t,t_o), \dots,$$

$$\phi_n(t,t_o) \Big]$$

where each of the columns satisfies the system of equations and the initial conditions are given by:

$$\phi(t_o,t_o) = I$$

An important property of the state transition matrix is $\phi(t,t_o) = \phi(t,t_1) \phi(t_1,t_o)$, the composition or semigroup property (11).

2.2 THE FLOQUET-LIAPUNOV THEOREM

Proof of the Floquet-Liapunov Theorem is given in References 10 and 11. The Theorem states that a system

such as Equation (2.1), with periodic coefficients, has tran-
sient solutions of the form

$$\{x(t)\} = \left[A(t)\right]\left[\diagdown e^{\Lambda t}\diagdown\right]\{\alpha\} \qquad (2.2)$$

where $A(t)$ is periodic with period T, Λ are complex
characteristic numbers and α are constants derived from
initial conditions. The stability of the system, therefore,
can be completely determined from the values of Λ. If
$\left[\phi(t)\right] = \phi(t,o)$ is a solution matrix, i.e. state transition
matrix, of the system whose columns are linearly independent
over the domain of the solution definition, the solution
can be written as:

$$\{x(t)\} = \left[\phi(t)\right]\{x(0)\} \qquad (2.3)$$

This fundamental matrix, $\phi(t)$, is defined such that

$$\left[\dot{\phi}(t)\right] + \left[D(t)\right]\left[\phi(t)\right] = 0$$

The Floquet Transition Matrix (FTM) is defined by

$$\{x(T)\} = \left[\phi(T)\right]\{x(0)\} \text{ where } \left[\phi(T)\right] = Q = FTM$$

It is shown in Reference 12 that by comparison of
Equations (2.2) and (2.3) one obtains

$$\left[A(0)\right]^{-1}Q\left[A(0)\right] = \left[\diagdown e^{\Lambda T}\diagdown\right]$$

which is the expression for an eigenvalue problem. Therefore,
$e^{\Lambda T}$ are the complex eigenvalues or characteristic multipliers
of the FTM, Q, and the columns of the matrix $A(0)$ are the
corresponding eigenvectors. A stable solution to Equation (2.1)
requires that the real part of Λ be negative. The use of

multivariable Floquet-Liapunov theory to develop the so-called
FTM method has been applied to several helicopter aeroelastic
stability problems (12-15).

The important consequences of this method are first, that
knowledge of the transition matrix over the period $0 \leq \psi \leq T$
determines the solution to Equation (2.1) everywhere because of
the composition property of the state transition matrix;
second, that knowledge of the transition matrix at the end
of the period determines the stability of the system. Other
advantages of the FTM method are that only one rotor revolution
of numerical integration (with initial condition of unity) for
each degree of freedom is necessary to define the FTM, Q.
Also, the ambiguous interpretation of time history response
data, which includes both forced and transient behavior, is
not necessary to determine stability.

2.3 MODAL DECOUPLING

Just as a system of linear, coupled, constant coefficient
equations can be uncoupled through a similarity transformation
so can a system of equations with periodic coefficients. The
procedure of solving the system of simultaneous differential
equations of motion by transforming them into a set of in-
dependent equations by means of the modal matrix is generally
referred to as modal analysis (16). Modal analysis can be
applied to the system in Equation (1) by making the variable
substitution:

$$\{x(t)\} = \left[A(t)\right]\{y(t)\}.$$

It can be shown the system in Equation (1) becomes:

$$\{\dot{y}(t)\} - [\diagdown\Lambda\diagup]\{y(t)\} = [A(t)]^{-1}\{f(t)\} = \{g(t)\}$$

These uncoupled constant coefficient equations can then be used to determine the forced response of the system (12).

The general case that has been addressed has been the case where the eigenvalues are distinct, which is the usual case for rotor stability and response problems. However, if the eigenvalues are not distinct the principles remain intact but the more complex Jordan form of a matrix, instead of a diagonal matrix, must be considered. This will not be discussed here.

While the modal functions obtained in the rotating system with periodic coefficients do not correspond directly to the mode shapes in the non-rotating system, this is not true for the damping characteristics. The real part of the complex eigenvalue correspond directly to the damping in the non-rotating system and can thus be correlated with measured damping.

3.   THE MATHEMATICAL MODEL

3.1   DESCRIPTION

The model is illustrated in Figure 3. It consists of a slender rigid blade, hinged at the center of rotation, with spring restraint at the hinge. The orientation of the flap (out-of-plane) and lag (in-plane) restraint springs which are parallel and perpendicular to the blade chord line, respectively, simulates the elastic coupling characteristics of the actual elastic blade. The spring stiffnesses are chosen so that the uncoupled rotating flap and lag natural frequencies coincide with the corresponding first mode rotating natural frequencies of the elastic blade. This allows the model to represent a hingeless rotor treated by virtual hinges or a fully hinged rotor (17).

The model chosen has been used to evaluate rotor aeroelastic stability and can include the incorporation of flap-lag elastic coupling, pitch-flap and pitch-lag coupling, and a blade lag damper. These were some of the fundamental dynamic mechanisms found important in the stability studies of References 13 and 18. Their importance to forced response is a major objective sought in this research.

The parameter R is defined so that flap-lag structural coupling may be included and may be varied to determine its effect on blade vibrations. Geometrically, it is defined as the ratio of the blade pitch angles inboard and outboard of the flap-lag hinge. Physically, it represents how the flap-lag structural coupling is dependent on the relative

stiffness of the blade segments inboard and outboard of the
pitch bearing. This is because the principal elastic axes
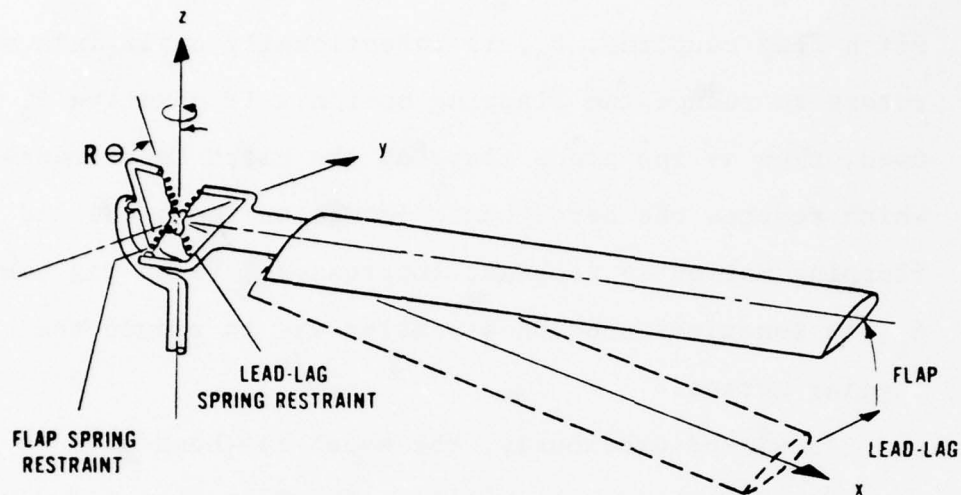
Figure 3.   Centrally Hinged, Spring Restrained,
Rigid Blade Representation

of the outboard segment rotate through an angle as the blade
pitch varies while the inboard segment principal axes do
not.   The method of implementation is accomplished by
replacing θ by $R\theta$ in the structural terms in the flap-lag
equations while the mass and inertial terms are unchanged.
Thus, when $R = 1$, the original equations are retained, but
as R is reduced to zero, the flap-lag structural coupling
terms diminish and eventually vanish (18).

Torsion is included in a quasi-steady manner as pitch-flap and pitch-lag coupling. This is accomplished by defining the pitch angle, θ, as:

$$\theta = \theta_o + \theta_s \sin\psi + \theta_c \cos\psi + \theta_\beta \, \delta\beta + \theta_\zeta \delta\zeta + \theta_\beta (\overline{\beta} - \beta_{pc}) + \theta_\zeta \overline{\zeta}$$

Pitch-flap coupling, θ_β, is intentionally built into some rotors to reduce the flapping motion. If negative θ_β is used, then as the blade flaps up the pitch is decreased, which reduces the aerodynamic forces on the blade and the flapping motion is somewhat suppressed. Pitch-lag coupling, θ_ζ, is sometimes used in a similar way to reduce the lagging motion.

As stated previously, the model has been used to evaluate aeroelastic stability. These studies (13,18), have shown the model to give quite reasonable accuracy at low advance ratios when compared with more complicated models. Since all pure helicopters currently developed operate at a $\mu < 0.5$ and the aeroelastic stability of a rotor is considered more sensitive to system parameters than forced response, the model is believed to be an adequate representation for parametric studies.

3.2 EQUATIONS OF MOTION

The general procedure followed was to derive the nonlinear flap-lag equations of a helicopter rotor in forward flight. The left hand side of the equations was made linear by considering small perturbation motions about a periodic equilibrium position (trimmed condition) of the nonlinear

system. The nonlinear terms were consolidated on the right hand side to form the following flap-lag perturbation equations of motion: (Appendix 9.2 gives the details of the derivation and a full set of equations.)

$$
\left\{ \begin{matrix} \delta\ddot{\beta} \\ \delta\ddot{\zeta} \end{matrix} \right\} + \left[C(\psi) \right] \left\{ \begin{matrix} \delta\dot{\beta} \\ \delta\dot{\zeta} \end{matrix} \right\} + \left[K(\psi) \right] \left\{ \begin{matrix} \delta\beta \\ \delta\zeta \end{matrix} \right\} = \left[L(\psi) \right] \left\{ \begin{matrix} \dot{\bar{\beta}} \\ \bar{\beta} \end{matrix} \right\} + \left[M(\psi) \right] \left\{ \begin{matrix} \bar{\theta} \\ \bar{\phi} \end{matrix} \right\} + \left[N(\psi) \right] \left\{ \begin{matrix} \ddot{\bar{\beta}} \\ C_{d_{o/a}} \end{matrix} \right\}
$$

There are two forms of periodic coefficients in the equations. First, there are the explicit periodic coefficients of the form $\mu \sin \psi$ or $\mu \cos \psi$. These types are only associated with aerodynamic terms. The second type are implicit periodic coefficients that result from the fact that $\bar{\theta}$ and $\bar{\beta}$ may have cyclic components. These types are found in both structural and aerodynamic terms. A damping term is included in the $C(\psi)$ matrix to account for the lead-lag damper included on many rotors, particularly hinged rotors. These equations are put into state variable format to reduce them to first order so that an efficient computer library differential equation solver can be utilized.

3.3 ASSUMPTIONS AND ORDERING SCHEME

The following basic assumptions are used to derive the flap-lag equations of motion used for the treatment of the aeroelastic stability and response problem:

(1) Aerodynamic forces are based on linear, quasi-steady strip theory; and induced flow is assumed to be

uniform and is obtained from simple momentum theory.

(2) Stall and compressibility effects are neglected.

(3) The rotor is trimmed according to the moment trim procedure described in a following section, or the rotor is left untrimmed. Any desired trimmed or equilibrium position can be duplicated by inputting the appropriate control settings.

(4) The rigid blade can only deflect in the flap and lead-lag directions and is torsionally rigid. However, the coupling effects of blade torsion are introduced through the coupling parameters R, θ_β, and θ_ζ.

(5) The blade geometric twist can also be represented by appropriately selecting values of the flap-lag coupling parameter, R.

(6) Structural and mechanical damping forces are assumed to be viscous.

(7) The deflections of the blade are moderately small so that terms of $0(\epsilon^2)$ can be neglected compared to one.

The flap-lag equations which define the mathematical model are obtained by writing equations for small perturbation motions about a periodic equilibrium motion of the nonlinear system. During this process one encounters a considerable number of terms which are small and therefore negligible. Therefore, a rational ordering scheme must be used which allows one to neglect terms in a systematic manner. The

scheme used is that of Reference 13 and is applied in the derivation in Appendix 9.2. The ordering scheme consists of assigning orders of magnitude to all important parameters of the problem in terms of a typical displacement quantity, ε_β. This results in neglecting higher order terms, $0(\varepsilon_\beta^2)$, with respect to unity in the $\delta\beta$ and $\delta\zeta$ coefficients, and by letting C_{d_o} and products of $\bar\beta$, $\bar\theta$, λ, and θ_ζ be neglected with respect to unity.

3.4 ADDITIONAL STRUCTURAL CONSIDERATIONS

In describing the model it was stated that both hinged and hingeless rotors could be represented. The relationships establishing this equivalency will be presented in this section. Another structural consideration is whether or not the lag hinge flaps with the blade. When the flap hinge is inboard of the lag hinge it flaps with the blade. If it is outboard of the lag hinge it does not. On a hinged rotor, the geometry of the mechanical hinges defines the kinematic relationship. On a hingeless rotor, it is more difficult to define the sequence of virtual hinges, especially if they are nearly coincident. This complicates the kinematic arrangement; and Reference 19 has shown that the hinge sequence of the blade has a marked influence on flap-lag stability. The sequence used in deriving the equations in Appendix 9.2 is lag-flap, i.e. the lag hinge does not flap with the blade. A relationship between the lag-flap and flap-lag sequences will be presented in this section, which allows the model to represent either kinematic relationship.

3.4.1 Equivalency of Hinged Rotors and Hingeless Rotors
Treated with Virtual Hinges

For a hinged rotor with both hinge offset, e, and a spring restraint, K_β, the dimensionless rotating flapping frequency is:

$$p = \left[1 + \frac{3}{2} \frac{e}{R-e} + \frac{K_\beta}{I_\beta \Omega^2} \right]^{1/2} \tag{3.1}$$

For a hingeless rotor, i.e. a cantilevered uniform blade, Rayleigh's method can be used to obtain Southwell's Equation (16). The first flapping mode can be calculated as:

$$p = \left[1.26 + \frac{12.39}{\Omega^2} \frac{EI}{\mu R^4} \right]^{1/2} \tag{3.2}$$

From Equations (3.1) and (3.2) one can set:

$$\left[1 + \frac{3}{2} \frac{e}{R-e} \right] = 1.26$$

and

$$3.52 \left(\frac{EI}{\mu R^4} \right)^{1/2} = \left(\frac{K_\beta}{\Omega^2 I_\beta} \right)^{1/2} \tag{3.3}$$

Hence, one can see that the cantilever blade is essentially the same as a hinged blade with offset and spring restraint. Therefore, K_β effective can be determined. A similar relationship can be expressed for the lagging frequencies. For zero offset, $K_\beta/\Omega^2 I_\beta = p^2-1$.

3.4.2 Relationship Between Lag-Flap and Flap-Lag Hinge
Sequences

The major difference between the lag-flap and flap-lag equations is the presence or absence of additional

pitch-lag and pitch-flap coupling terms (19). These differences are illustrated in the velocity component perpendicular to the plane of rotation, $\overline{U}_p$.

For a lag-flap sequence:

$$\overline{U}_p = \lambda + \overline{r}\dot{\beta} + \mu\beta c\psi - \mu\beta\zeta s\psi \tag{3.4}$$

For a flap-lag sequence:

$$\overline{U}_p = \lambda + \overline{r}\dot{\beta} + \mu\beta c\psi + \overline{r}\beta\zeta \tag{3.5}$$

When these expressions are substituted into the flap aerodynamic force, $\overline{F}_\beta$, and integrated along the blade the following coefficients of $\beta\zeta$ are obtained:

For flap-lag: $\quad \dfrac{\gamma}{8}\left[-1 - \dfrac{4}{3}\mu s\psi - 2\mu^2 c^2\psi \right] \beta\zeta \tag{3.6}$

For lag-flap: $\quad \dfrac{\gamma}{8}\left[\dfrac{4}{3}\mu s\psi + 2\mu^2 s^2\psi - 2\mu^2 c^2\psi \right] \beta\zeta \tag{3.7}$

The perturbation expansion $\beta\zeta$ results in retention of only the $\overline{\beta}\delta\zeta$ term. By defining a parameter, RFL, the model and flap-lag equations derived in Appendix 9.2 can be used for a flap-lag or a lag-flap sequence. This is accomplished by retaining terms from both Equations (3.6) and (3.7) in the $K(\psi)$ matrix. Thus, the following term is added:

$$\text{RFL} \left[\frac{\gamma}{8}(1 + \frac{8}{3}\mu s\psi + 2\mu^2 s^2\psi) \right] \overline{\beta}\delta\zeta \tag{3.8}$$

where:

$$\text{RFL} = 0 \text{ (lag-flap)}$$
$$1 \text{ (flap-lag)}$$

The parameter RFL is an input parameter to the main computer program (Appendix 9.3). Hingeless rotors can be modeled by choosing RFL between zero and one, depending upon the configuration.

Since $\overline{U}_p$ is also present in the lag aerodynamic force, $\overline{F}_\zeta$, similar $\beta\zeta$ expressions are obtained. These terms are handled as above. The following terms are added in the $K(\psi)$ matrix:

$$\text{RFL} \left[\frac{\gamma}{8}(1 + \frac{8}{3}\mu s\psi + 2\mu^2 s^2\psi)\overline{\theta} \right] \overline{\beta}\delta\zeta \tag{3.9}$$

$$-\text{RFL} \left[\frac{\gamma}{8}(3\overline{\phi}\mu s\psi + \frac{8}{3}\dot{\overline{\beta}}\mu s\psi - 4\mu^2 s\psi c\psi) \right] \overline{\beta}\delta\zeta \tag{3.10}$$

$$-\text{RFL} \left[\frac{\gamma}{8}(2\overline{\phi} + 2\dot{\overline{\beta}} + \frac{8}{3}\mu c\psi\overline{\beta}) \right] \overline{\beta}\delta\zeta \tag{3.11}$$

4. METHOD OF SOLUTION

4.1 EIGENVALUE AND MODAL DECOUPLING ANALYSIS

The method used to solve the linearized flap-lag
equations with periodic coefficients is called an eigen-
value and modal decoupling analysis. It takes advantage of
Floquet Theory with its application to linear systems with
time varying coefficients. It is unique in that it extends
the Floquet Transition Matrix (FTM) Method (12) to include
the calculation of forced response. The eigenvalue and
modal decoupling method is summarized in Table 1. Once the
flap-lag equations have been put into state variable format,
the state transition matrix and FTM are obtained by step-wise
integration over one period. This period consists of one
rotor revolution from time zero to 2π. Once the FTM, $\Phi(T)$,
is obtained it can be shown by application of the Floquet-
Liapunov Theorem (12) that the problem of stability reduces
to solution of an eigenvalue problem. Stability is deter-
mined from the real part of the complex eigenvalue, $\Lambda = \eta + i\omega$.
Therefore, when η is negative the system is stable, with
$\eta = 0$ representing the stability limit or boundary.

The extension of the FTM Method to determine forced
response requires considerable manipulation although the
mathematics are relatively simple. The eigenvectors of the
FTM and the state transition matrix at each integration step
increment must be obtained and saved. This is necessary in
order that the characteristic functions, $A(t)$, can be

calculated and used as a variable substitution to decouple the system of equations. This procedure is completely analogous to the modal analysis method (16) used to uncouple a system of equations with constant coefficients. Hence, the name eigenvalue and modal decoupling analysis is given to the method of solution.

4.2 CALCULATION OF HUB SHEARS AND MOMENTS

The information obtained from the analysis are the flap and lag displacements and velocities. These quantities are combined in the time domain to obtain flap and lag shears and moments in both the rotating and non-rotating systems. Once calculated, the shears and moments are harmonically analyzed through Fourier Series expansion to determine the relative strengths of the rotor harmonics. In the rotating system, the primary concern is fatigue of root end and hub components so that the first harmonic (1/REV) is the major oscillatory source. In the fixed system, the rotor acts as a filter and only allows rotor harmonics that are integral multiples of the number of blades to be transmitted. Therefore, for a two bladed helicopter only the even harmonics, 2/REV, 4/REV, etc. are of major concern in the fixed system. The root shears and moments for each blade in the rotating coordinate system are expressed as the integrals of the blade aerodynamic and inertial loading. The single-bladed results in the fixed system are valid for rotors with any number of blades so long as the appropriate solution harmonics are set to zero. Therefore, if a three bladed rotor is

being analyzed only the 3/REV loads are of interest in the
fixed system. The expressions for the hub shears and
moments in the rotating and fixed systems are given in
Table 2. Derivation of these expressions is given in
Appendix 9.2.

TABLE 1

Eigenvalue and Modal Decoupling Analysis

Step	Computation

1   Put Flap-Lag Equations into State Variable Format:
$$\{\dot{x}(t)\} + [D(t)]\ \{x(t)\} = \{f(t)\}$$

2   Determine the State Transition Matrix, $[\phi(t)]$, and
FTM, $[Q]$, by Numerical Integration Over One Period:
$$\{x(t)\} = [\phi(t)]\ \{x(0)\},\ [Q] = [\phi(T)]$$

3   Find Eigenvalues and Eigenvectors of FTM:
$$[A(0)]^{-1}\ [Q][A(0)] = [\ ^\diagdown e^{\Lambda T}\ ],\ [\ ^\diagdown\Lambda\ ] = [\ ^\diagdown\eta\ ] + i\ [\ ^\diagdown\omega\ ]$$

4   Obtain the Characteristic Functions, $[A(t)]$, for
Variable Substitution, $\{x(t)\} = [A(t)]\ \{y(t)\}$, for
Each Time Increment:
$$[A(t)] = [\phi(t)]\ [A(0)]\ [\ ^\diagdown e^{-\Lambda t}\ ]$$

5.   Compute Inverse Matrix, $[A(t)]^{-1}$, to Obtain:
$$[A(t)]^{-1}\ \{f(t)\} = \{g(t)\}$$

TABLE 1 (Cont'd)

6   Obtain the Uncoupled Equations by Variable Substitution:

$$\left[A(t)\right]\{\dot{y}(t)\} + \left(\left[\dot{A}(t)\right] + \left[D(t)\right]\left[A(t)\right]\right)\{y(t)\} = \{f(t)\}$$

$$\{\dot{y}(t)\} + \left(\left[A(t)\right]^{-1}\left[\dot{A}(t)\right] + \left[A(t)\right]^{-1}\left[D(t)\right]\left[A(t)\right]\right)\{y(t)\} = \{g(t)\}$$

$$\{\dot{y}(t)\} - \left[\diagdown \Lambda \diagdown\right]\{y(t)\} = \{g(t)\} = \sum_{n=-\infty}^{+\infty}\{a\}_n e^{int}$$

7   Obtain $y(t)$ From Complex Fourier Analysis:

$$\{y(t)\} = \sum_{n=-\infty}^{+\infty}\left[\diagdown \frac{1}{in-\Lambda}\diagdown\right]\{a\}_n e^{int}$$

8   Obtain $\{x(t)\}$ From Matrix Multiplication, $\{x(t)\} = \left[A(t)\right]\{y(t)\}$, and Convert $\{x(t)\}$ Information in Time Domain to Vibratory Shears and Moments

9   Fourier Analyze Shears and Moments to Obtain Strength of Harmonic Components

TABLE 2

Expressions for Hub Shears and Moments

Component	Expression
Flap Shears (Rotating):	$\overline{C}_{V\beta} = \frac{1}{\gamma}\int_0^1 \overline{F}_\beta d\overline{r} - \frac{1.5}{\gamma}\ddot{\beta}$
(Fixed):	$\left(\overline{C}_{V\beta}\right)_F = -\overline{C}_{V\beta}$
Lag Shears (Rotating):	$\overline{C}_{V\zeta} = \frac{1}{\gamma}\int_0^1 \overline{F}_\zeta d\overline{r} - \frac{1.5}{\gamma}\ddot{\zeta} + \frac{3}{\gamma}\beta\dot{\beta}$ $-\frac{2}{\gamma}(DPL)(ZSC)\omega_\zeta\dot{\zeta}$

(Fixed)

(Forward): $\quad \bar{x} = \bar{C}_{V\zeta} \sin\psi + (\bar{C}_{V\beta}\cos\psi)\beta - \frac{3}{8}\cos\psi\ \dot{\zeta}$

$$- \frac{1.5}{\gamma}\dot{\beta}^2\cos\psi$$

(Right): $\quad \bar{y} = \bar{C}_{V\zeta}\cos\psi - (\bar{C}_{V\beta}\sin\psi)\beta + \frac{3}{\gamma}\dot{\zeta}\sin\psi$

$$+ \frac{1.5}{\gamma}\dot{\beta}^2\sin\psi$$

Flap Moments

(Rotating): $\quad \bar{C}_{S\beta} = \frac{p^2-1}{\gamma}\ \beta + \frac{Z}{\gamma}\zeta$

(Fixed)

(Pitch): $\quad \bar{C}_M = -\ \bar{C}_{S\beta}\cos(\psi)$

(Roll): $\quad \bar{C}_L = -\ \bar{C}_{S\beta}\sin(\psi)$

Lag Moments

(Rotating): $\quad \bar{C}_{S\zeta} = \frac{Z}{\gamma}\beta + \frac{1}{\gamma}\omega_\zeta^2\zeta + \frac{2}{\gamma}(DPL)\omega_\zeta\dot{\zeta}$

4.3 MOMENT TRIM PROCEDURE

In this study, the nonlinear equations of motion developed in the previous sections are transformed into linear perturbation equations about a time dependent equilibrium position which is determined from a trimmed or untrimmed position of the helicopter in forward flight. In the trimmed and untrimmed procedures the rotor is maintained at a fixed value of thrust coefficient with forward flight. This procedure simulates actual forward flight conditions of a helicopter.

For the trimmed condition, a moment trim procedure was utilized which specifies that zero pitching and rolling moments on the rotor are maintained simulating conditions under which a rotor would be tested in the wind tunnel. The equations used to calculate the control settings necessary to maintain zero pitching and rolling moments for a given thrust setting are given in Reference 20. These equations are obtained by a closed form harmonic balance method applied to the flapping equation of motion.

Equations are also developed in Reference 20 for the untrimmed condition, i.e. β_s, $\beta_c \neq 0$. These equations are used to study the stiff inplane hingeless tail rotors in Section 6. Provisions have also been incorporated to input any desired control settings into the main computer program described in Section 5. This allows simulation of a flight condition obtained from test or another analysis. Correlation with the hypothetical rotor of Reference 3 was obtained using this procedure.

5.   COMPUTATIONAL PROCEDURES

5.1   DESCRIPTION OF MAIN PROGRAM

The computer program written to implement the Eigen-value and Modal Decoupling Method consists of twenty-three subroutines and one main calling routine. A qualitative description of the main program flow paths is shown in Table 3.   Numerous options are available for evaluating sweeps of several parameters and trimmed or untrimmed solutions. In addition, the structure of the program is such that the order of the system may be increased by simply changing only two or three subroutines. For completeness, a listing of the main program is included in Appendix 9.3.

5.2   DESCRIPTION OF SUBROUTINES

The subroutines used in the program were obtained from various sources. The majority come from the IBM Scientific Subroutine Package (SSP), although many of these were modified to accommodate the specific problem. Other sub-routines were written to calculate the hub shears and moments. A description of each subroutine, where it was obtained, and how it is used in the program is included in Appendix 9.3.

TABLE 3. Main Program Flow Chart
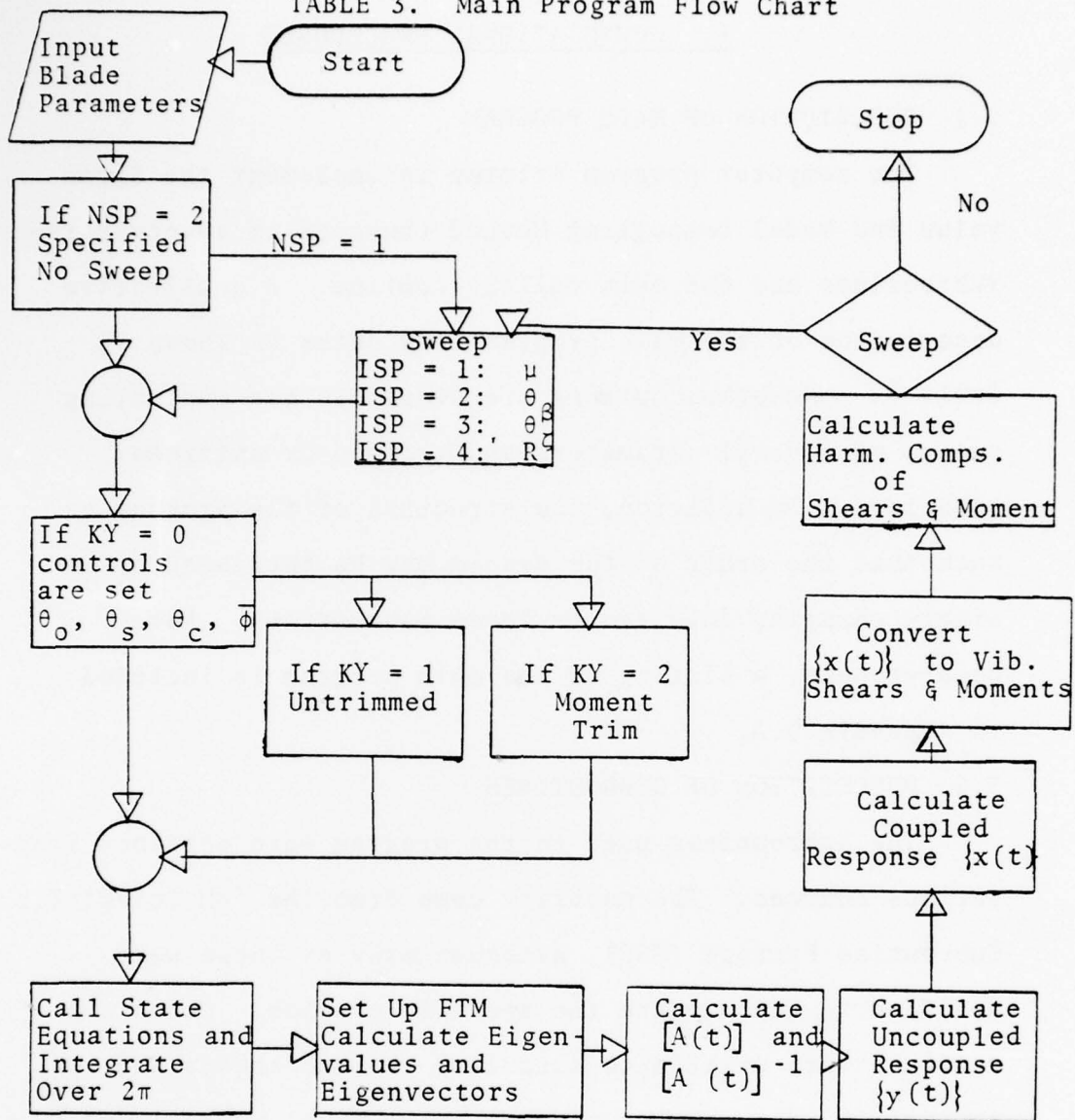
6. RESULTS AND DISCUSSION

As with any new analytical method, correlation with
other proven analyses or with measured data must be obtained
for validation. The comparison study of Reference 3 and
test data from the UTTAS Program are used for this purpose.
Four different rotors are studied: the hypothetical hinged
rotor of Reference 3, a soft inplane hingeless (HL) main
rotor, and two stiff inplane hingeless (flexstrap) tail
rotors. The rotor blade input parameters for the baseline
case for each of these rotors are presented in Table 4.

Three different procedures are used in obtaining the equi-
librium position about which the perturbation expansions are
made. For the hinged rotor No. 1, the control settings are
obtained from Reference 3 and input into the main computer
program. For the soft inplane rotor No. 2, a moment trim
condition is obtained that utilizes the trimmed equations
of Reference 20 (which have been incorporated in the main
computer program). Since tail rotors are not trimmed in
actual flight, the untrimmed equations of Reference 20 are
utilized for the two stiff inplane hingeless rotors, Nos.
3 and 4. The untrimmed equations also have been incorporated
in the main computer program. In all four cases, the baseline
configuration corresponds to a high speed forward flight
condition. To study the effect of structural parameters on
the flap-lag forced response and stability of a rotor blade
in forward flight, sweeps on $\mu, \theta_\beta, \theta_\zeta$, R, and DPL are made

TABLE 4

Rotor Blade Input Parameters

No.	1	2	3	4
Type	Hinged	HL(Soft)	HL(Stiff)	HL(Stiff)
p	1.031	1.136	1.16	1.08
ω_ζ	0.25	0.75	1.67	1.51
γ	7.5	9.3	2.9	2.4
R (elastic)	0	0	0	0
RFL	0	0	1	1
DPL	.15	0	0	0
θ_β	0	-.15	-.70	-2.1
θ_ζ	0	0	0	0
β_{pc}	0	.06	0	0
C_T	.0063	.0062	.0068	.0068
C_{d_o}	.010	.010	.013	.013
R (feet)	25.	24.5	5.5	5.0
b	3.	4.	4.	4.
c (feet)	1.83	1.92	0.81	0.59
σ	.07	.10	.19	.19
Function	Main Rotor	Main Rotor	Tail Rotor	Tail Rotor
Controls	Specified	Moment Trimmed	Un-Trimmed	Un-Trimmed
$\theta_{pre-coupled}$	0	0	.131	.157
ZSC	0	0	0	0
μ	0.33	0.36	0.42	0.42

from the baseline configurations. While all four rotors are
analyzed in great detail, particular emphasis is placed on
the two stiff inplane hingeless (flexstrap) tail rotors since
they include large variations in the important structural
coupling parameters; and since they come closest to the
assumed blade model. The important results for each rotor
will be presented in the subsequent sections.

6.1 HINGED ROTOR RESULTS

The first rotor in Table 4 is typical of hinged rotors
on current operational helicopters. It includes a lag damper,
as do most hinged rotors, to insure freedom from mechanical
instability, usually called ground resonance. Since the
rotor has three blades, the third harmonic (3/REV) is the
largest source of vibration in the fixed system. However,
this 3/REV vibration is caused by 2/REV, 3/REV, and 4/REV
shears and moments in the rotating system. The first harmonic
(1/REV) forces in the rotating system are most important when
considering blade and hub component fatigue lives.

Calculated hub vertical and horizontal shears are com-
pared in Figures 4 and 5 with the results of Reference 3.
While considerable variation among all the analyses is
evident, the results obtained with the eigenvalue and
modal decoupling method, labeled FL for flap-lag, compare
favorably with the larger and more sophisticated methods.
The major discrepancies are found in the 3/REV horizontal
shears. For the higher harmonics, the blade elasticity
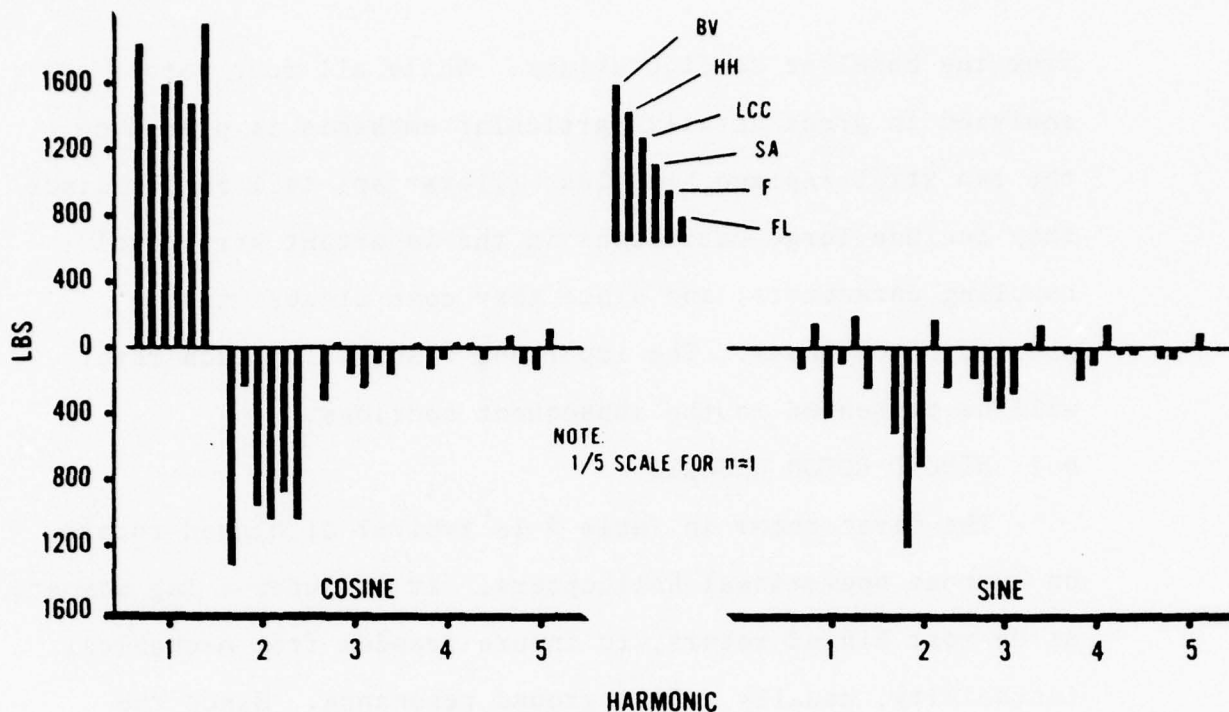
Figure 4. Hub Vertical Shears, Rotor No. 1

naturally plays an important role; and the rigid blade
analysis is inadequate. Despite this inadequacy, however,
the present results fall generally within the scatter of
the other analyses.

The variation of flap and lag shears with advance ratio,
forward speed, is illustrated in Figures 6 and 7. These
figures clearly illustrate how rotor loads can limit
forward flight performance. Blade root and hub components
must be built to withstand these high speed vibratory loads.
For these calculations, with linear aerodynamics, the n per
rev shears scale as μ^n. This is an important simplification
and could be used to extrapolate loads to other flight speeds.
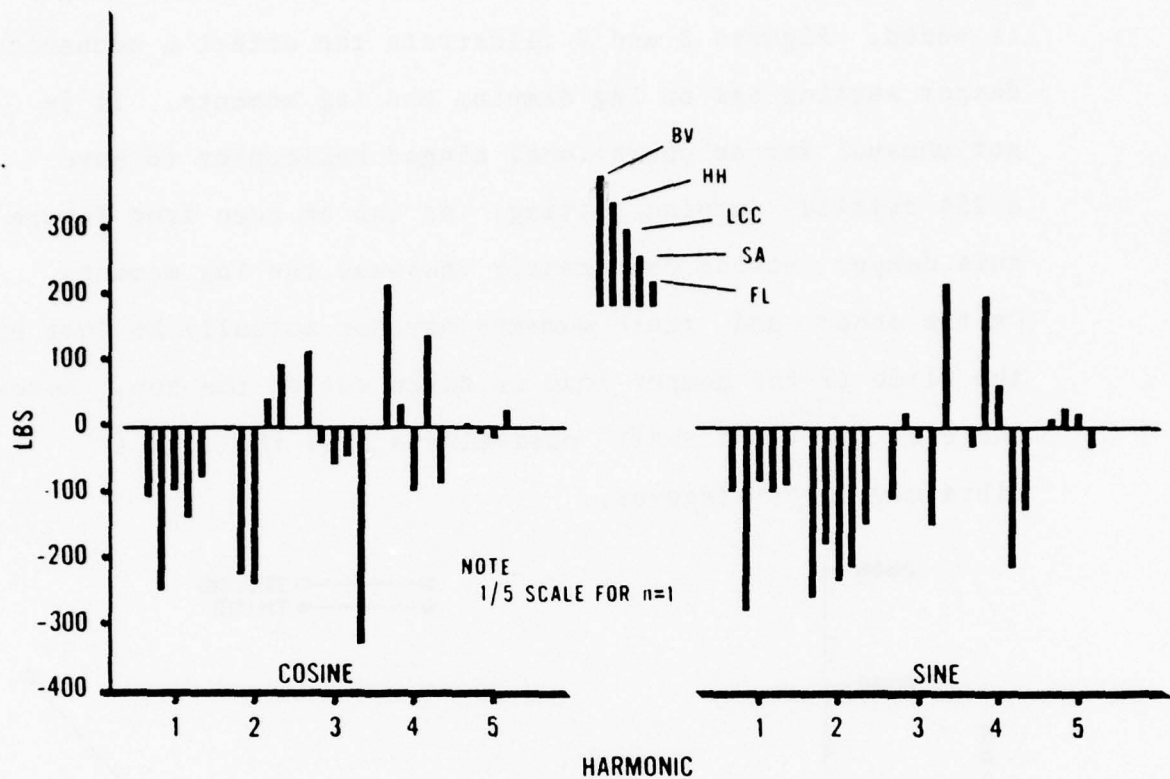
Figure 5. Hub Horizontal Shears, Rotor No. 1

It must be noted, however, that the extrapolation would
only hold valid in the cruise range (.05 < μ < 0.25 for main
rotors and .05 < μ < .50 for tail rotors). The transition
wake at lower speeds and stall at higher speeds would
violate the present assumptions.

Blade lag dampers are considered essential for hinged
rotors to insure freedom from mechanical instability.
Coalescence between the blade lag motion and the helicopter
rolling or pitching motion is the source of this instability.

Since the lag motion is lightly damped a mechanical damper
is added. Figures 8 and 9 illustrate the effect a mechanical
damper setting has on lag damping and lag moments. It is
not unusual for an operational hinged helicopter to have
a 25% critical damping setting. As can be seen from Figure 9,
this damper setting can greatly increase the lag moments.
On the other hand, these moments may not actually be felt by
the blade if the damper load is taken out at the hub. Never-
theless, the rotor shaft must always feel the load as
vibratory shaft stresses.
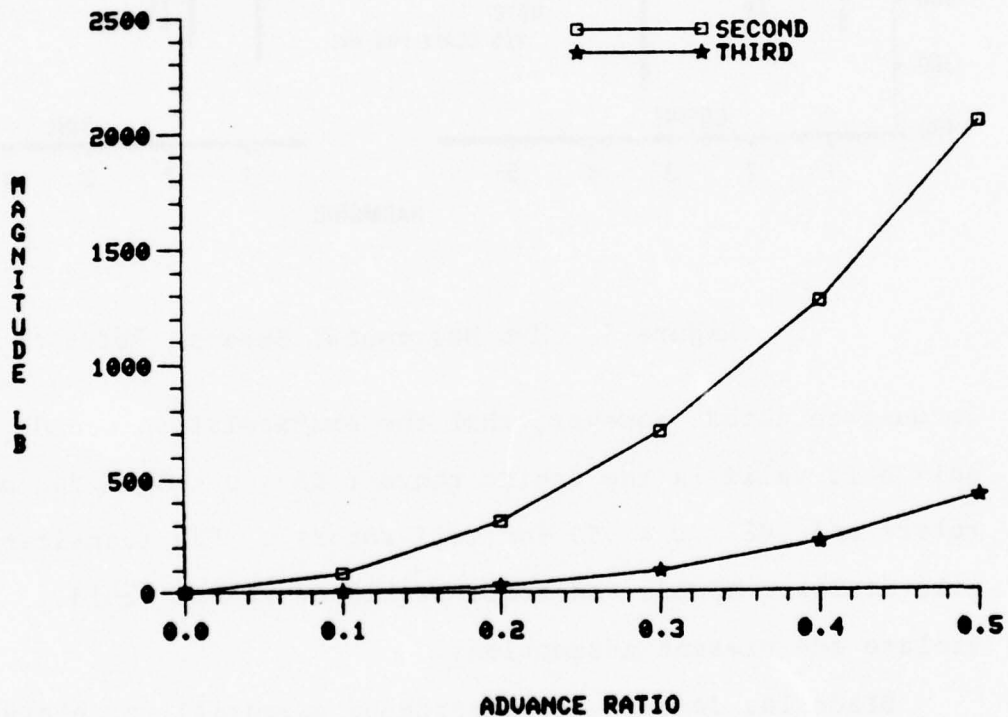
Figure 6. Flap Shears vs Advance Ratio, Rotor No. 1
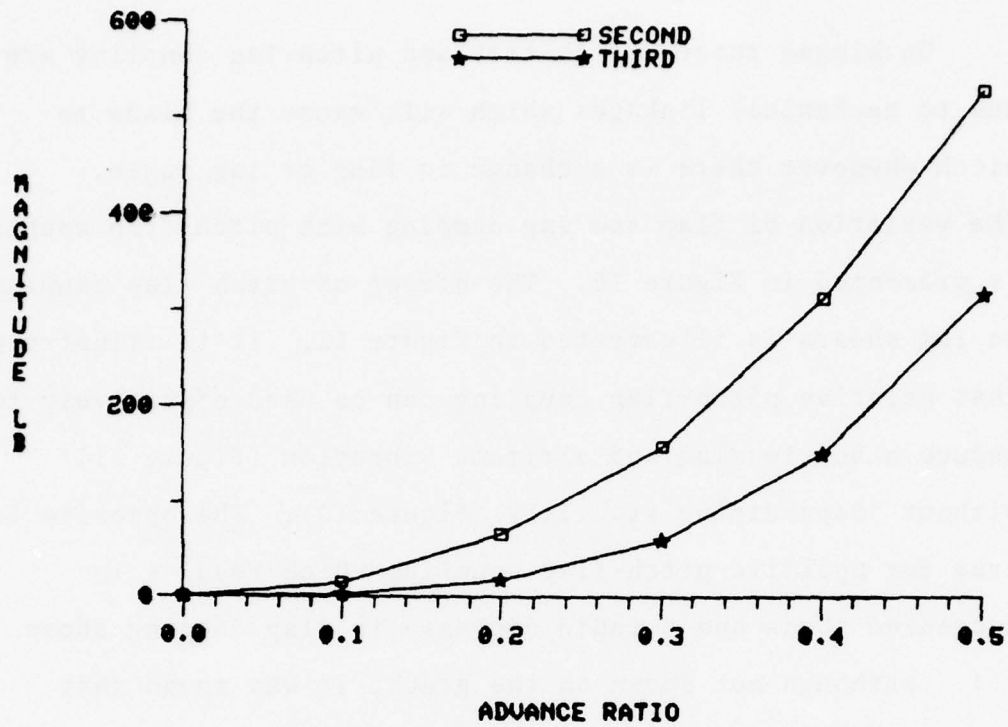
Figure 7.   Lag Shears vs Advance Ratio, Rotor No. 1
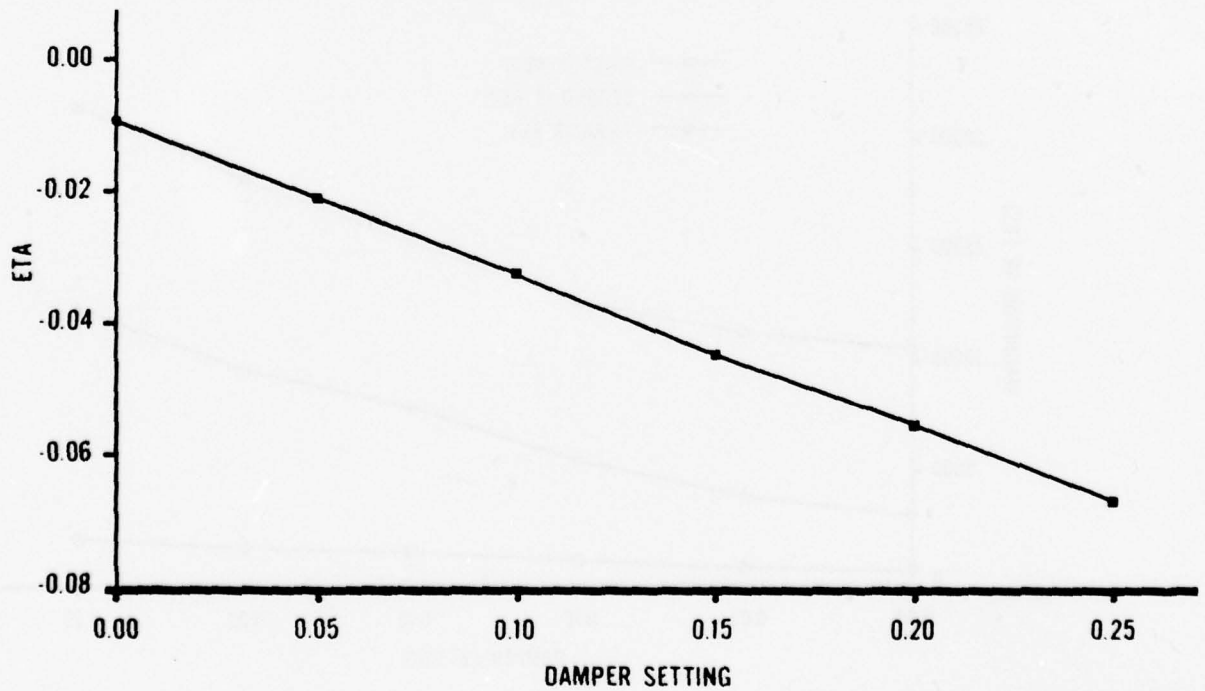
Figure 8.   Lag Damping vs Damper Setting, Rotor No. 1

On hinged rotors pitch-flap and pitch-lag coupling are
due to mechanical linkages which will cause the blade to
pitch whenever there is a change in flap or lag angle.
The variation of flap and lag damping with pitch-flap coupling
is presented in Figure 10. The effect of pitch-flap coupling
on lag shears is illustrated in Figure 11. It is illustrated
that negative pitch-flap coupling can be used effectively to
reduce blade loading and airframe vibration (Figure 11)
without jeopardizing stability (Figure 10). The opposite is
true for positive pitch-flap coupling which results in
increased loads and a rapid decrease in flap damping above
0.4. Although not shown on the graph, it was found that
θ_β had a much smaller effect on 2 and 3/REV flap shears.
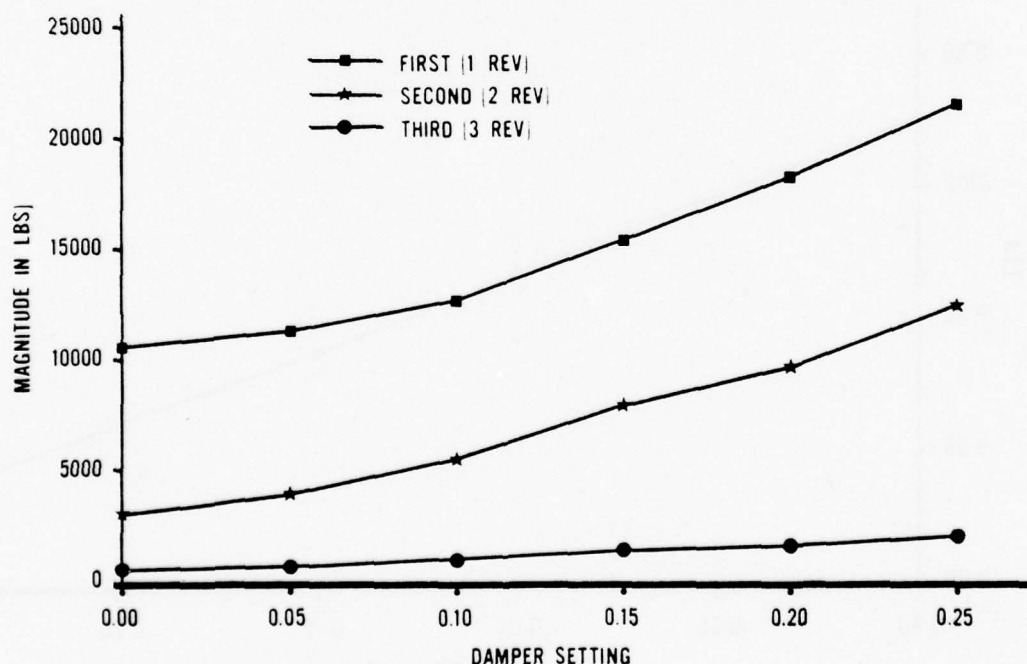
Figure 9. Lag Moments vs Damper Setting, Rotor No. 1
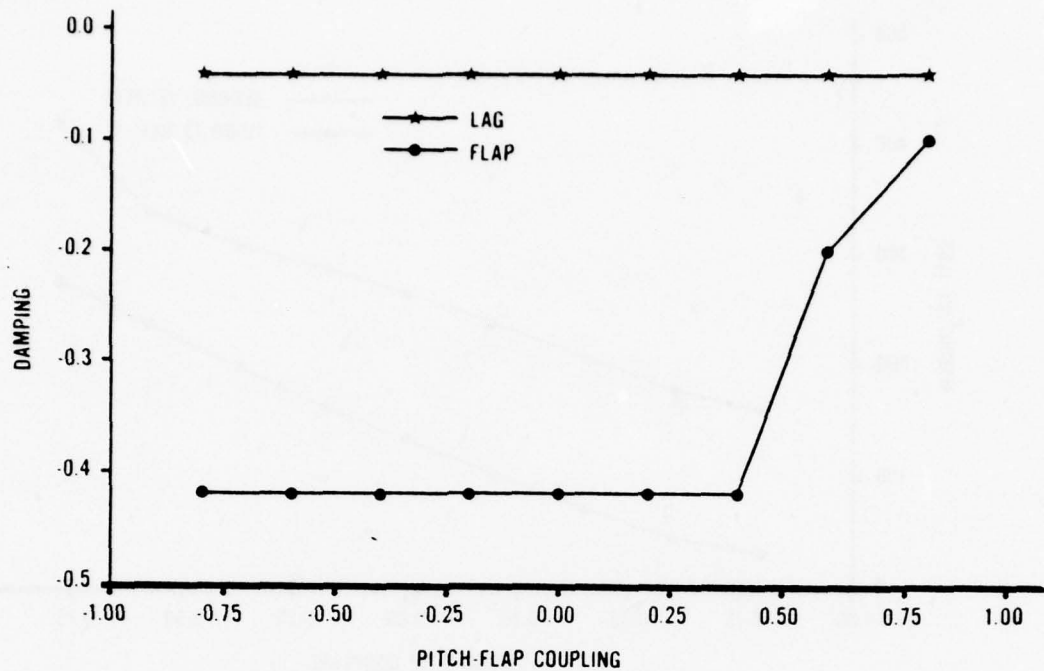
Figure 10. Damping vs Pitch-Flap Coupling, Rotor No. 1

Pitch-lag coupling effects are shown in Figures 12 and
13. It appears that little benefit is gained with respect
to either loads or vibration. Lag damping varies greatly with
pitch-lag coupling. The flattening out of the damping curve
in Figure 12 for positive pitch-lag coupling is due to the
15% critical damping setting for the baseline configuration
(Table 4.). Pitch-lag coupling, θ_ζ, also had little effect
on flap shears.
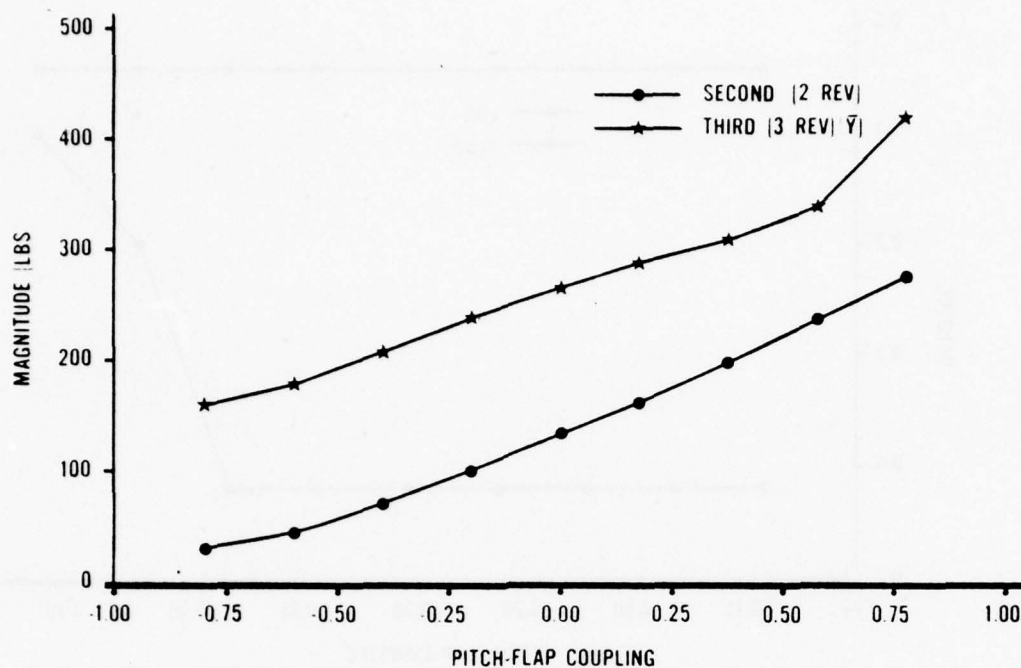
Figure 11. Lag and Lateral Shears vs Pitch-Flap Coupling, Rotor No. 1
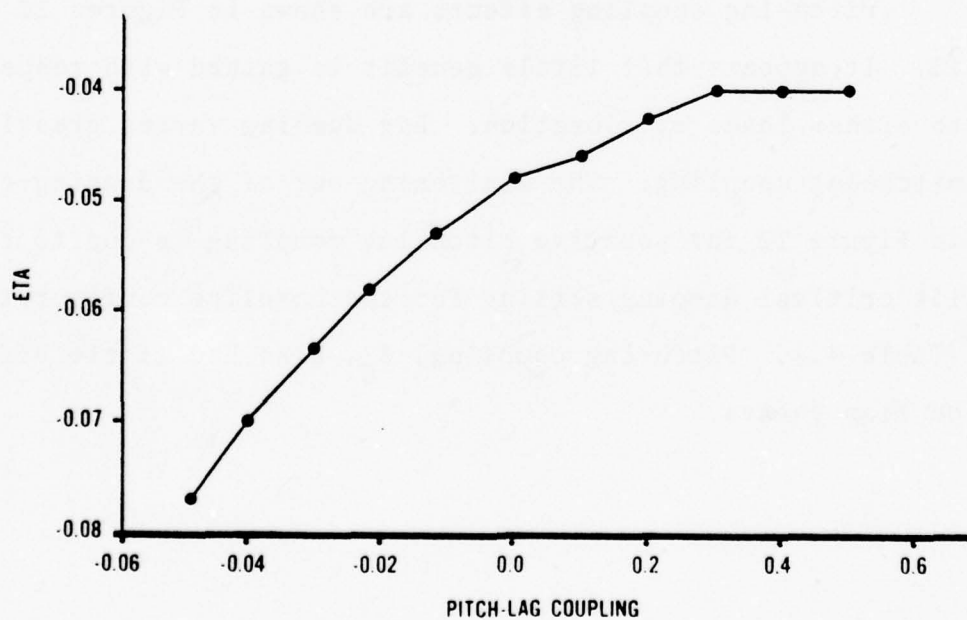
Figure 12. Lag Damping vs Pitch-Lag Coupling, Rotor No. 1
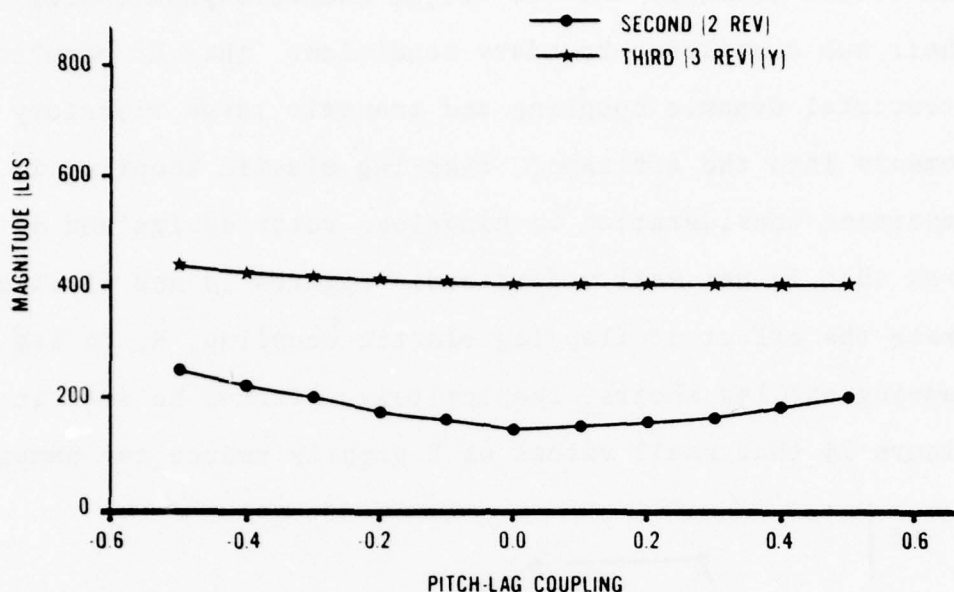
Figure 13. Lag and Lateral Shears vs Pitch-Lag Coupling, Rotor No. 1

6.2 HINGELESS (SOFT IN-PLANE) ROTOR RESULTS

The second rotor in Table 4 is called hingeless because it has no mechanical hinge to allow flapping or lagging motion as does the hinged rotor. The term "soft inplane" hingeless rotor is often applied because the frequency in the plane of rotation (lag) is less than the rotor speed (1/REV). This rotor includes β_{pc} and θ_β in its baseline configuration. Since the rotor has four blades, the first five rotor harmonics can be considered critical in the rotating system. This rotor is very similar to one of the UTTAS candidate helicopters.

Hingeless rotors are attractive because they increase the helicopter's control power, simplify the rotor mechanically,

and reduce somewhat the hub weight and aerodynamic drag. With
their hub cantilever boundary conditions, they do complicate
structural dynamic coupling and transmit large vibratory rotor
moments into the airframe. Flap-lag elastic coupling is an
important consideration in hingeless rotor design and is an
area that is not well understood. Figures 14 and 15 illus-
trate the effect of flap-lag elastic coupling, R, on lag
damping and lag shears, respectively. It can be seen in
Figure 14 that small values of R greatly reduce lag damping
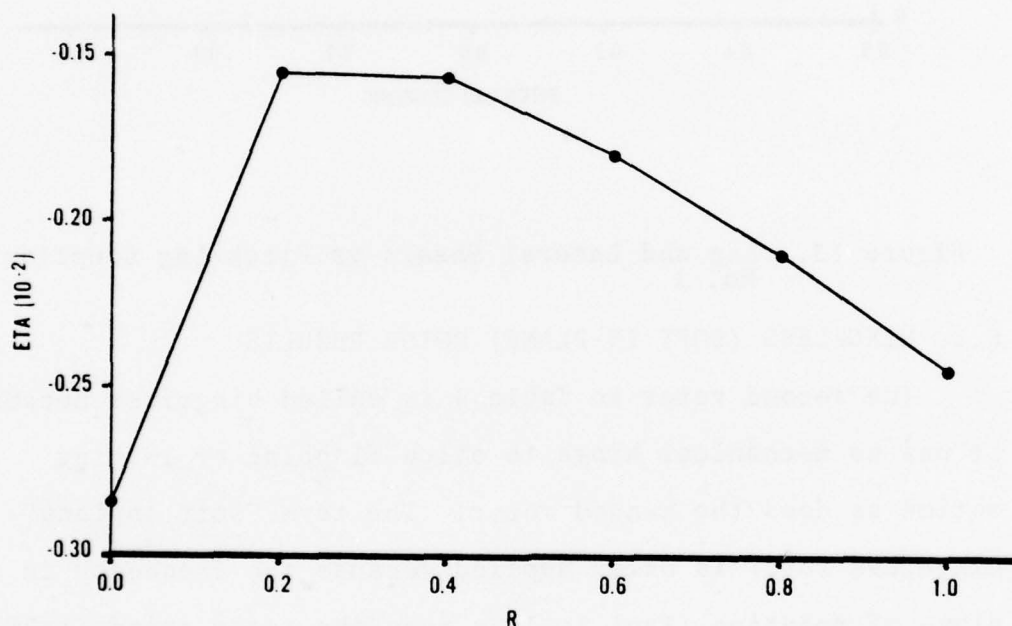
Figure 14. Lag Damping vs Elastic Coupling, R, Rotor No. 2

but that the trend is reversed for larger values of R. Thus,
there is a least stable value of R near 0.25. This phenomenon
has been pointed out in Reference 13. With respect to lag
shears; the 1/REV shears are reduced as R approaches zero, but
they are relatively constant for larger values of R.

The variations with respect to pitch-flap and pitch-lag coupling are similar to the trends found for the hinged rotor. Figure 16 illustrates the reduction in flap damping with positive pitch-flap coupling. For a positive value of 1 the flap damping is reduced to almost zero, the stability boundary. This instability is a parametric 0.5/REV resonance that can occur when too much θ_β is used. For large positive pitch-lag coupling (Figure 17) the lag damping becomes positive, indicating an instability. If no lag damper had been installed on the hinged rotor a similar trend would have been expected. On the other hand, negative θ_ζ is highly stabilizing at no penalty to vibrations.
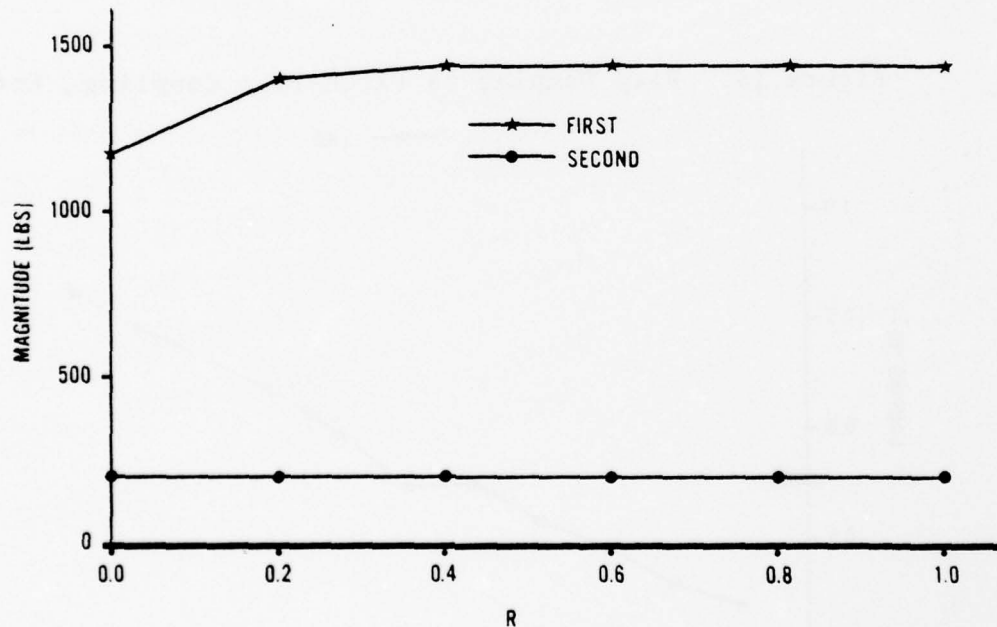
Figure 15.   Lag Shears vs Elastic Coupling, R, Rotor No. 2
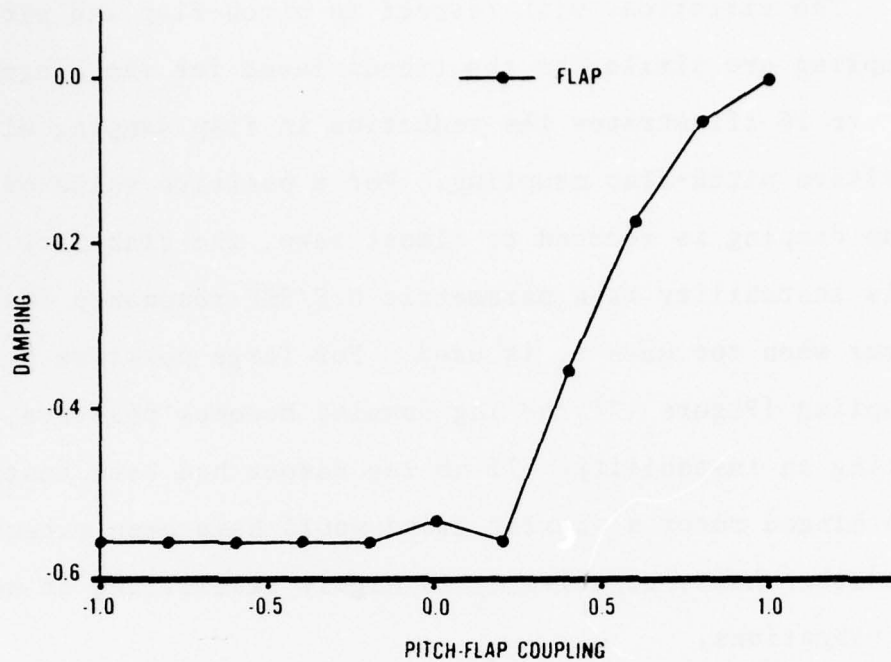
Figure 16.   Flap Damping vs Pitch-Flap Coupling, Rotor No. 2
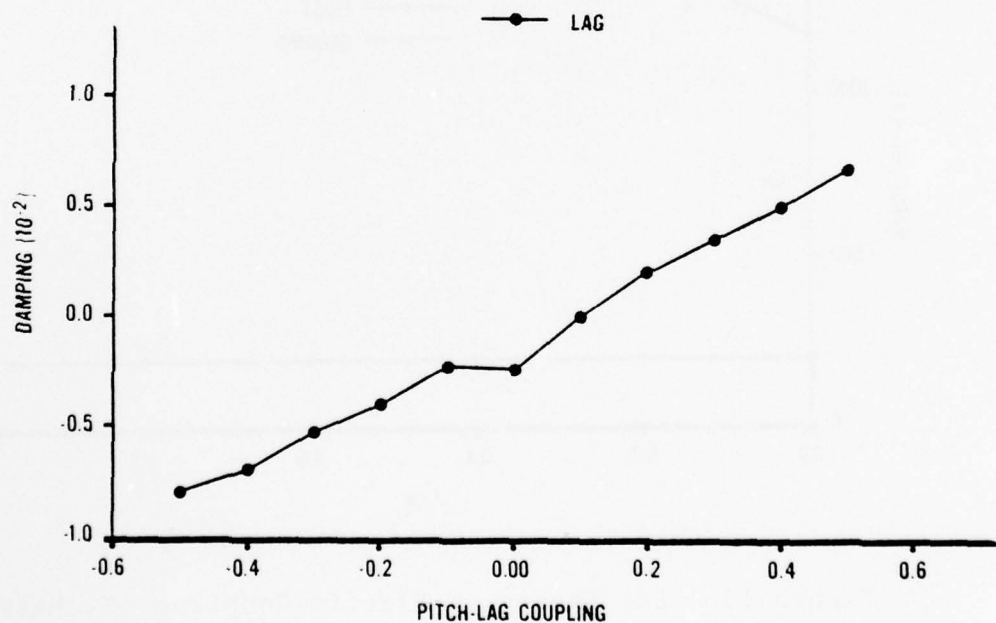
Figure 17.   Lag Damping vs Pitch-Lag Coupling, Rotor No. 2

6.3 HINGELESS (STIFF IN-PLANE) ROTOR RESULTS

The last two rotors in Table 4 are classified as "stiff inplane" because their lag frequencies are greater than the rotor speed (1/REV). In addition, they are classified as flexstrap rotors because the opposing rotor blades are retained by a flexible strap or beam. Over the past several years, there has been a popular trend toward the increased usage of bearingless helicopter rotors for both main and tail rotors (22). A flexstrap rotor accomplishes this by introducing pitch through strap twist, thus allowing the removal of the pitch bearing, the only bearing usually retained on hingeless rotors. The bearingless rotor is less complex, has fewer parts and joints, is lighter, and requires less maintenance (23).   There have been two major drawbacks to the development of bearingless rotors. First, such designs can include large variations in aeroelastic and structural couplings which can lead to aeroelastic instabilities. Second, the materiel selected for the flexstrap must be able to withstand the large vibratory stresses associated with a hingeless rotor. The two rotors analyzed are similar to the two UTTAS candidates' tail rotors. Both rotors went through several years of development which included model and full scale wind tunnel tests, whirl tower tests, and numerous analyses. Summaries of these development programs are given in References 22 and 23.

The two drawbacks mentioned in the last paragraph make the eigenvalue and modal decoupling method an excellent tool

for studying the tradeoffs necessary to design such a rotor.
In addition, since most of the flexibility of the flexstrap
rotor is at the root of the blade, the mathematical model
of Figure 3 lends itself well to this type rotor. The
results for each rotor are presented and discussed in the
following sections.

6.3.1 Flexstrap Tail Rotor No. 1

The baseline configuration for this rotor, No. 3 in
Table 4, includes -35° of pitch-flap coupling (tan -35° = -.70)
which is approximately 33% the pitch-flap coupling of the
second tail rotor i.e. -65° (tan -65° = -2.1). It is stated
in Reference 22 that the larger pitch-flap coupling in the
second tail rotor was necessary to reduce flap bending loads
in forward flight. While no pitch-lag coupling was included
mechanically in either configuration, significant pitch-lag
coupling can result from the pitch-flap coupling introduced.
A change of pitch angle with lagging angle can arise from a
mechanical or effective tilt of the lag hinge with respect
to the spanwise axis or a torsional moment which twists the
blade when the blade is deflected in the flapping or lagging
directions (21). It has been shown in Reference (21) that
the amount of torsional moment is directly proportional to
the differences in the inverses of the flap and lag blade
stiffnesses. For a "matched-stiffness" blade the torque due
to blade deflection will be zero, however, for "stiff in-plane"
hingeless rotors this configuration is almost impossible to

achieve. For the two tail rotors differences in lag and flap stiffnesses, i.e. $\omega_\zeta^2 - \omega_\beta^2$, of 1.02 and 2.12 are achieved, respectively. These differences are also indicative of the influence of flap-lag elastic coupling.

Correlation with measured loads is presented in Figure 18. The curve labeled TEST was obtained during a flight load survey which was part of the UTTAS development program. The hump in the test data at low speed flight can be attributed to nonuniform, transition inflow. The hump at the high speed flight can be attributed to blade stall. Since both of these effects have been neglected in the analysis it is felt that excellent correlation has been achieved for the flapping moments. Thus, one would expect qualitative agreement of the present results with flight data for 1/rev loads at cruise speeds. The analysis curve in Figure 18 was achieved by summing the first four harmonics of the blade flap moment. The remaining results for both tail rotors are presented in a nondimensional form to enhance their general applicability. Since the major concerns with tail rotor vibratory loads are the fatigue lives of blade and hub components the 1/REV loads will normally be presented.

The variation of flap and lag shears and moments with advance ratio are illustrated in Figure 19. It can be seen that the 1/REV loads vary in more of a linear fashion with advance ratio than did the higher harmonics in earlier figures. Even though the flap shears have been reduced by

a factor of ten to illustrate the variation of all loads, it is the flap moments that are the major concern of design engineers.
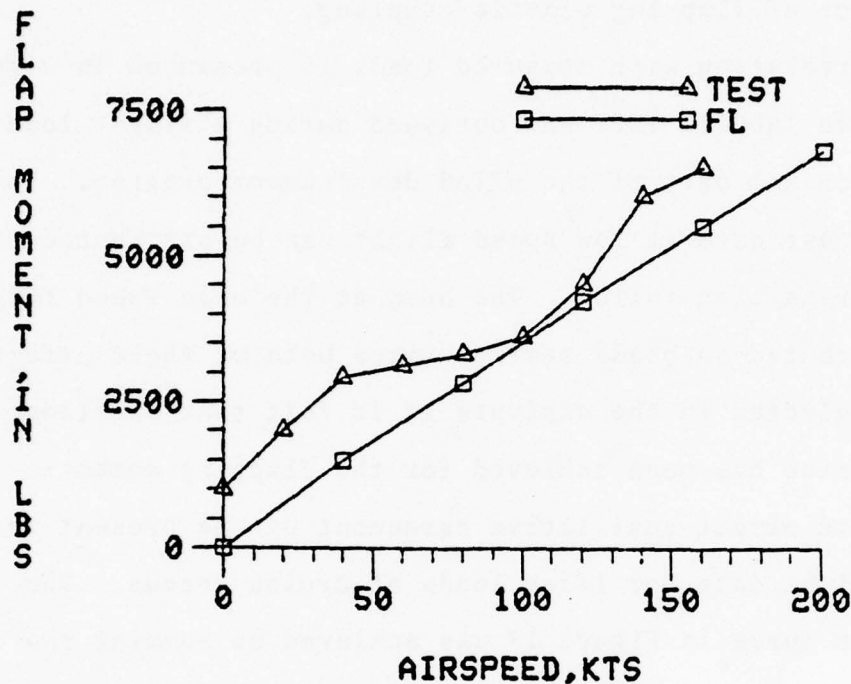
Figure 18.   Correlation Between Flight Test Data and Analysis, Rotor No. 3

Flap-lag elastic coupling, R, is an important parameter for hingeless rotors. While no attempt was made to give a specific value to the baseline configuration its effect on forced response and stability was obtained by sweeping R from zero to one. An advance ratio of 0.42 which corresponded to the maximum level flight speed was used as the baseline for all the parameter sweeps. The effect of R is illustrated in Figures 20 and 21. Lag damping is increased considerably with R while flap damping is slightly decreased (Figure 20).
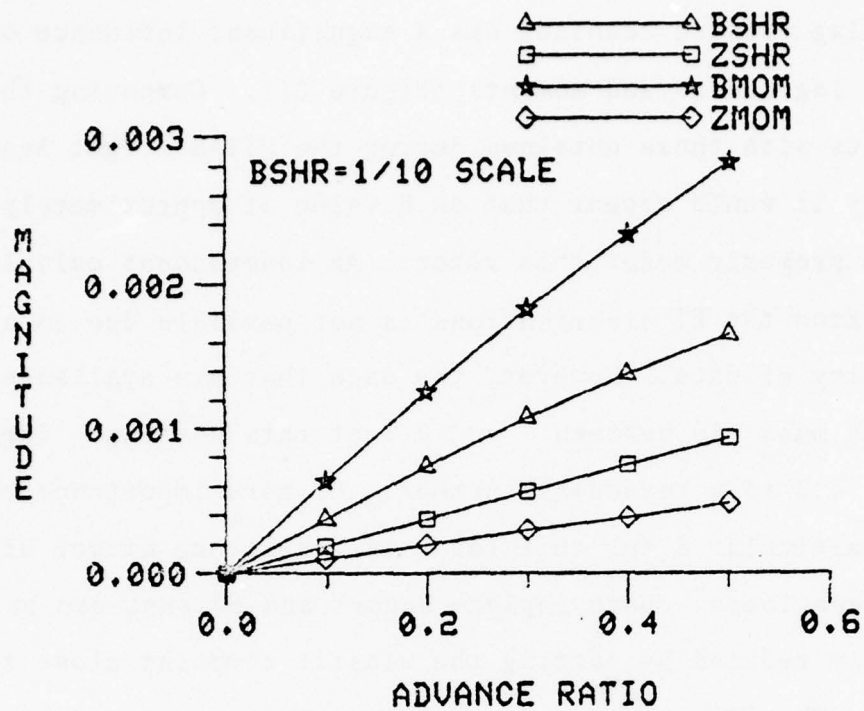
Figure 19. Variation of 1/REV Rotor Loads with Advance Ratio, Rotor No. 3
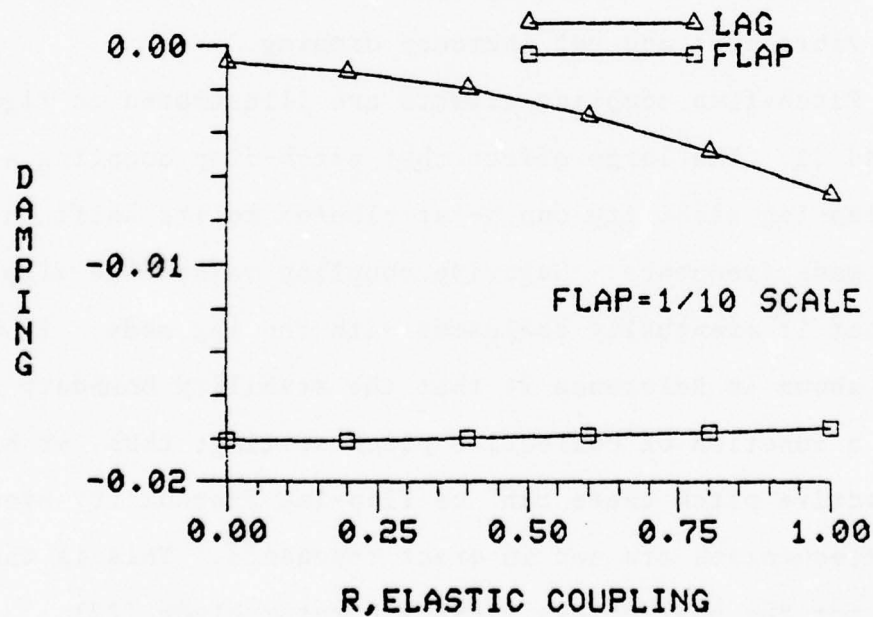
Figure 20. Variation of Damping with Elastic Coupling, Rotor No. 3

Flap-lag elastic coupling has a significant influence on 1/REV lag shears and moments (Figure 21). Comparing the lag moments with those obtained during the UTTAS flight loads survey it would appear that an R value of approximately 0.2 would properly model this rotor. An independent calculation of R from the EI distributions is not possible due to a scarcity of data. However, the data that are available shows that R must lie between 0 and 0.5 at this setting. Therefore, 0.2 is a reasonable number. Of more importance than the particular R for this rotor is the strong effect of R on blade loads. Both inplane shears and moments can be greatly reduced by setting the elastic coupling close to zero. The flap shears and moments, however, are unchanged by moving to R = 0; and the inplane damping is deteriorated. Therefore, elastic coupling alone could not be used to minimize vibrations and yet increase damping.

Pitch-flap coupling effects are illustrated in Figures 22 and 23. The large effect that pitch-flap coupling has on flap-lag stability can be attributed to its shift in flap mode frequency. Negative coupling raises the flap mode so that it eventually coalesces with the lag mode. It has been shown in Reference 24 that the stability boundary is also a function of collective pitch setting; thus, at higher collective pitch there can be flap-lag instability even if the frequencies are not in exact resonance. This is the case for the bearingless flexstrap rotor blade (22).
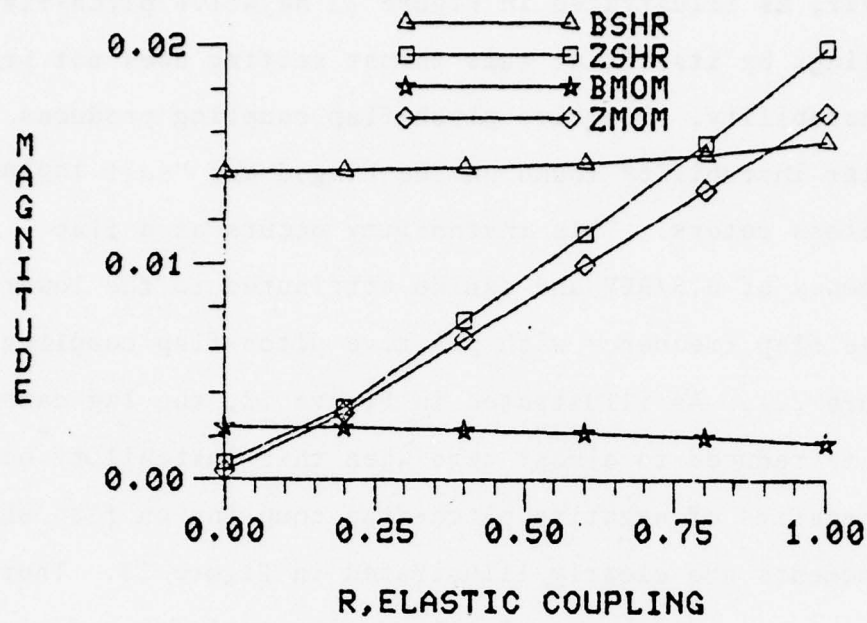
Figure 21. Variation of 1/REV Rotor Loads with Elastic Coupling, Rotor No. 3
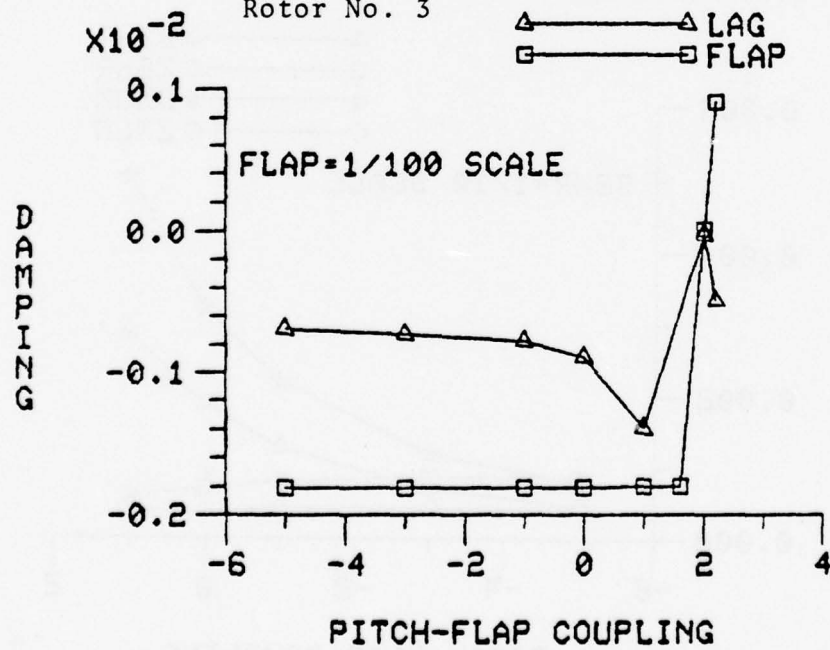
Figure 22. Variation of Damping with Pitch-Flap Coupling, Rotor No. 3

However, as illustrated in Figure 22 negative pitch-flap coupling, by itself, at this thrust setting does not produce an instability. Positive pitch-flap coupling produces a similar instability found on the hinged and "soft inplane" hingeless rotors. This instability occurs at a flap frequency of 0.5/REV and can be attributed to the lowering of the flap frequency with positive pitch-flap coupling (Figure 22). As illustrated in Figure 22, the lag damping also is reduced to almost zero when this instability occurs. The benefits of negative pitch-flap coupling on flap shears and moments are clearly illustrated in Figure 23. Therefore, negative θ_β could be a valuable design tool for reducing 1/REV flapping shears and moments while leaving damping and inplane loads unchanged.
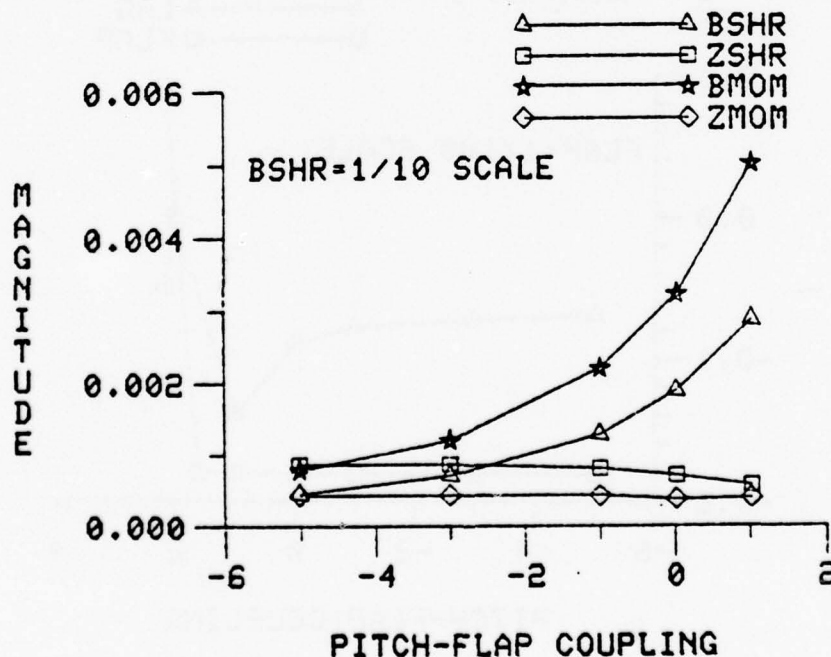
Figure 23. Variation of 1/REV Rotor Loads with Pitch-Flap Coupling, Rotor No. 3

Pitch-lag coupling effects are illustrated in Figures 24 and 25. While lag damping steadily decreases with negative coupling, it appears that sufficient damping is available for the pitch-flap coupling of 35° chosen for the baseline configuration tan (-35°) = -.70. Pitch-lag coupling appears to have little influence on rotor loads (Figure 25). Therefore, pitch-lag coupling could be used as a powerful design tool to stabilize a system without deteriorating its vibrational characteristics.

6.3.2 Flexstrap Tail Rotor No. 2

The baseline configuration for this rotor, No. 4 in Table 4, is similar to Tail Rotor No. 1 except for the much larger pitch-flap coupling and smaller Lock number, γ. Sweep was included in the final prototype version but was not included in this analysis. The two tail rotors operate at different rotor speeds, 1214 RPM for Tail Rotor No. 1 and 1337 RPM for Tail Rotor No. 2. Therefore, the advance ratio of .42 used for the sweeps of Tail Rotor No. 1 would correspond to a different forward flight speed for Tail Rotor No. 2; however, for direct comparison purposes it was set at .42 for the sweeps of Tail Rotor No. 2.

The variation of 1/REV rotor loads with advance ratio is illustrated in Figure 26. Comparing these loads with those in Figure 19 reveals the beneficial effects of the increased pitch-flap coupling on flap moments and shears. The loads in Figure 26 are much smaller than their counterparts in Figure 19.
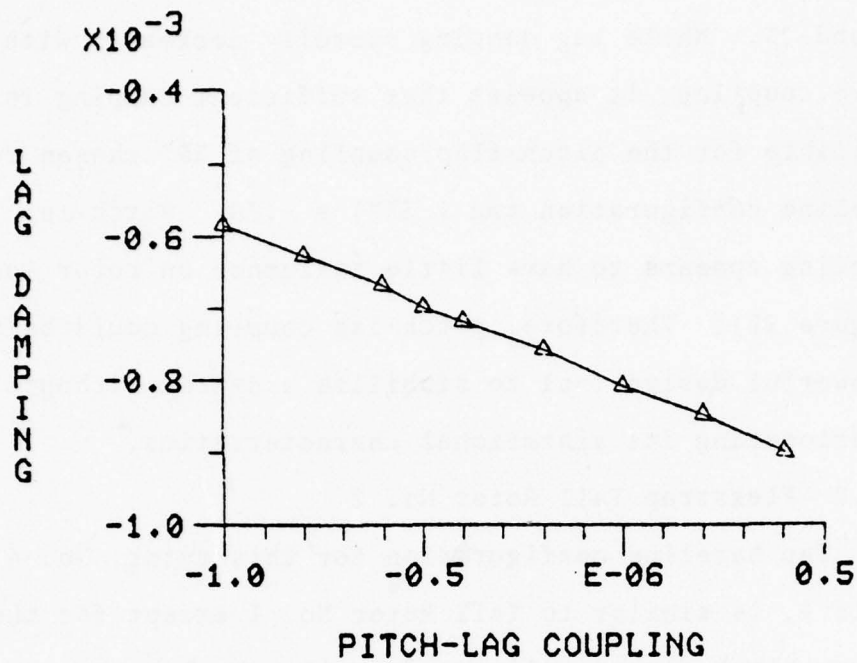
Figure 24.   Variation of Lag Damping with Pitch-Lag Coupling, Rotor No. 3
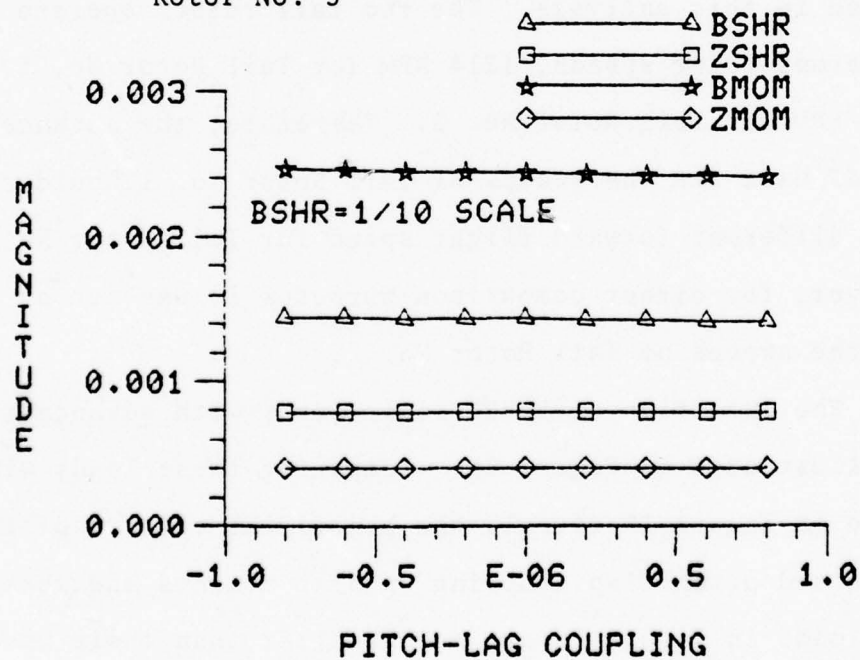
Figure 25.   Variation of 1/REV Rotor Loads with Pitch-Lag Coupling , Rotor No. 3

Pitch-flap coupling effects are more clearly illustrated in Figures 27, 28, and 29. While the baseline configuration includes -65° of pitch-flap coupling, θ_β = -2.14, it is stated in Reference 22 that the elastic pitch-flap coupling is actually equivalent to -72.5°, θ_β = -3.17. At this value the first flap frequency in air is 1.42/REV (22). Figure 27 illustrates the variation in flap and lag frequencies with pitch-flap coupling. The flap frequency at -3.17 is approximately equal to 1.42/REV, which agrees with Reference 22. Coalescence of the flap and lag modes occurs at a pitch-flap coupling of approximately -3.5 (Figure 27). Also illustrated is the reduction of the flap frequency to 0.50/REV at a pitch-flap coupling of 2.2 (Figure 27).

The rapid reduction of flap damping at large positive pitch-flap coupling is illustrated in Figure 28. It is also interesting to note the slight decrease in flap damping at a lower positive pitch-flap coupling (0.4). This is where the flap frequency in Figure 27 crosses 1/REV. As observed with Tail Rotor No. 1, there appears to be no flap-lag instability caused by negative pitch-flap coupling in itself. Figure 29 shows the large reductions in flap moments and shears gained with negative pitch-flap coupling. Figure 29 also shows, as did Figure 23, the effectiveness of negative θ_β is limited. For θ_β < - 5.0, little further improvement is made. It must also be stated that overly large negative θ_β can destabilize higher bending modes.
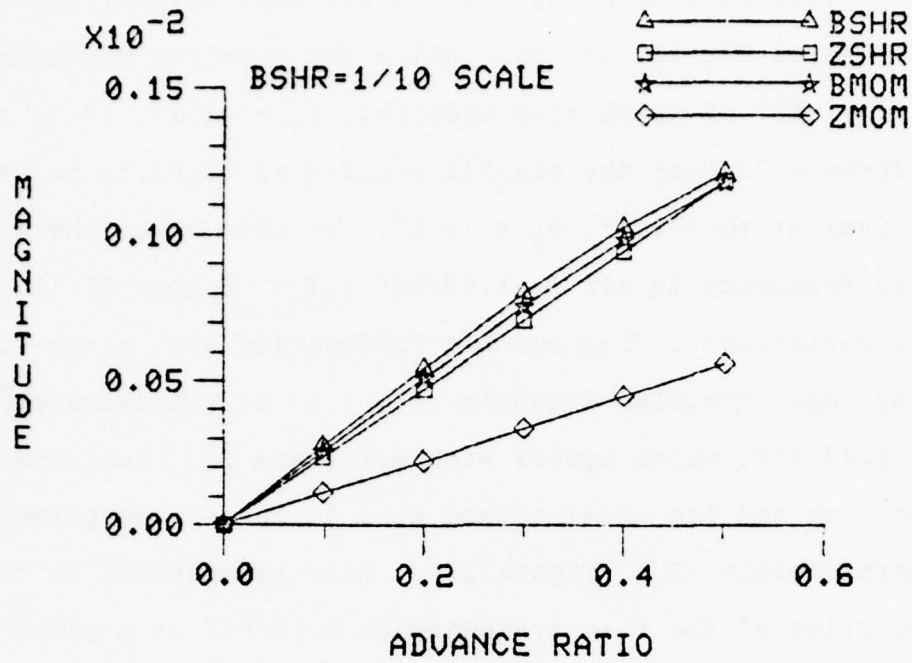
Figure 26. Variation of 1/REV Rotor Loads with Advance Ratio, Rotor No. 4
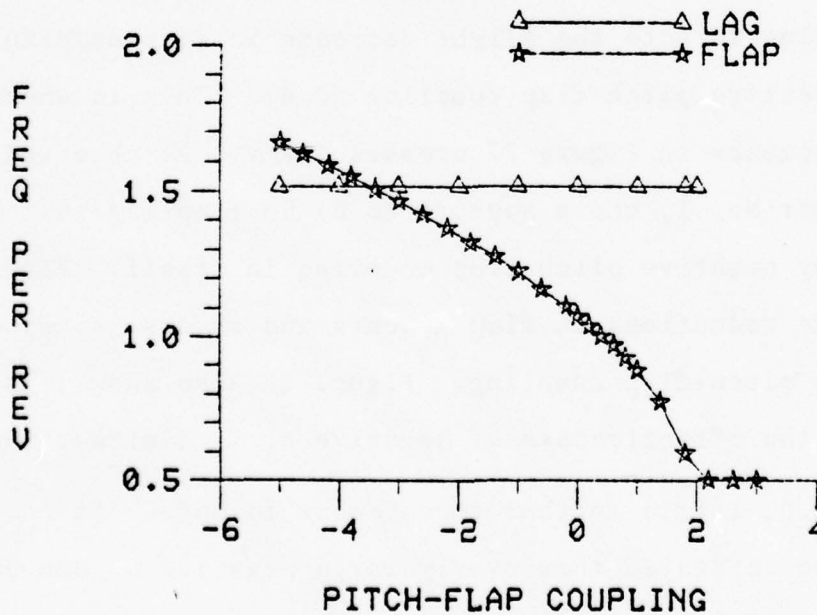
Figure 27. Variation of Frequencies with Pitch-Flap Coupling, Rotor No. 4
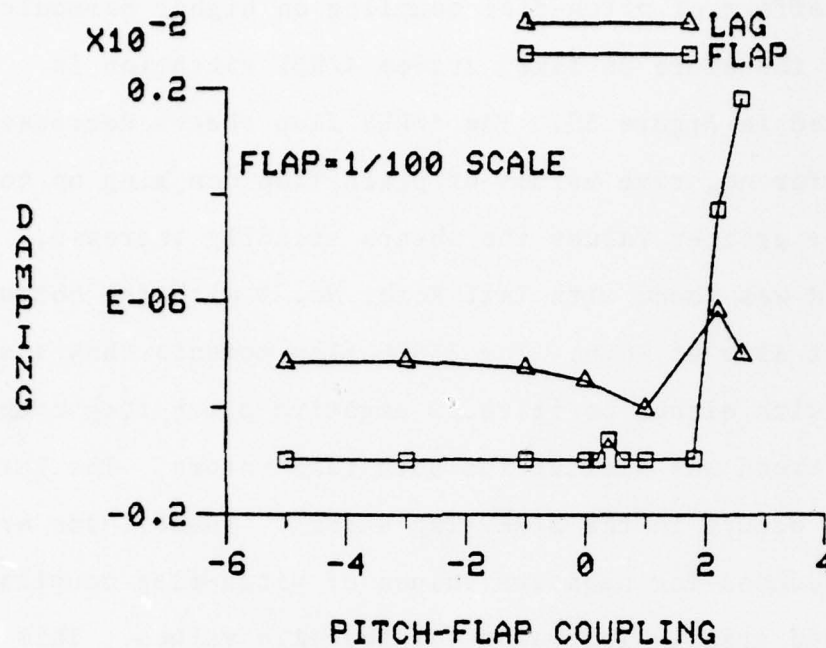
Figure 28.   Variation of Damping with Pitch-Flap Coupling,
             Rotor No. 4
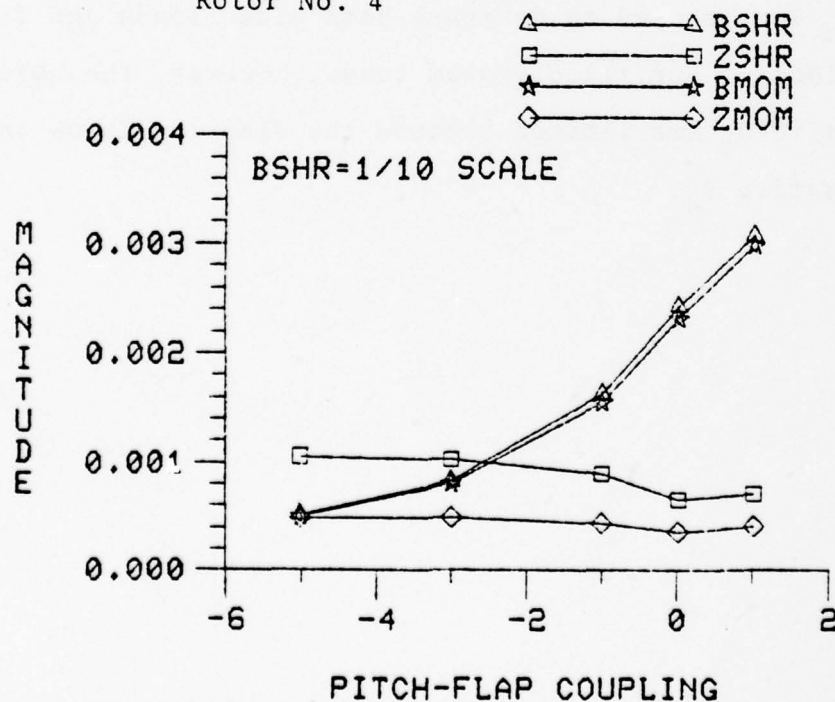
Figure 29.   Variation of 1/REV Rotor Loads with Pitch-Flap
             Coupling, Rotor No. 4

The effect of pitch-flap coupling on higher harmonic loads and therefore on fixed system 4/REV vibration is illustrated in Figure 30. The 4/REV flap shears decrease slightly for negative values of pitch-flap coupling up to -0.6. For greater values the shears steadily increase. The same trend was found with Tail Rotor No. 1 with the bottom of the bucket also at -0.6. The 3/REV flap moments show a steady increase with either positive or negative pitch-flap coupling and this trend was similar for both tail rotors. The largest variation occurs in the 3/REV lag shears. These loads are greatly reduced for negative values of pitch-flap coupling up to -2.0 and greatly increased for positive values. This trend was also found true for the hinged rotor (Figure 11). There-fore, θ_β can be used to decrease both blade loads and fixed system loads. For fixed system loads, however, the benefits of negative θ_β are limited because the flapping loads increase with negative θ_β.
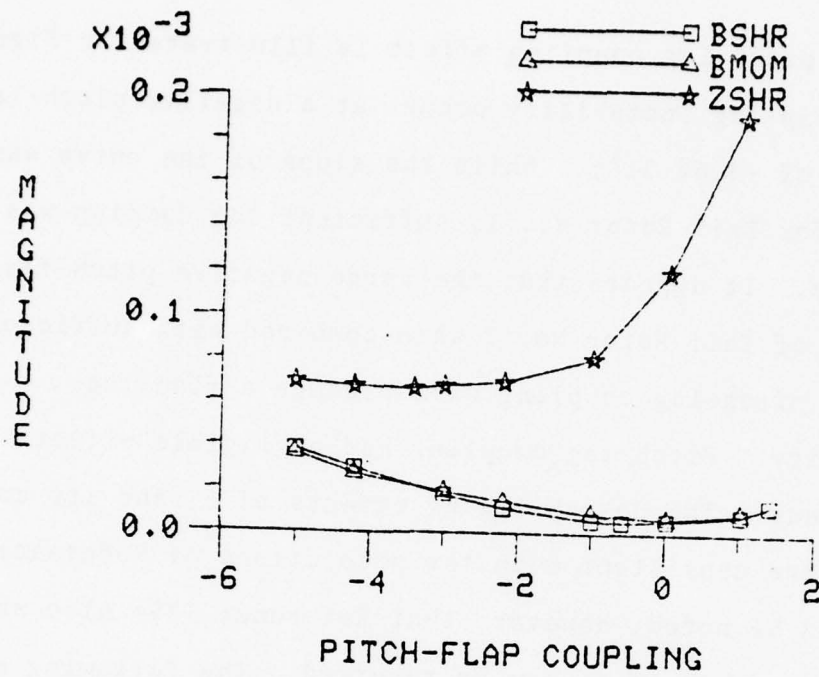
Figure 30.   Variation of Higher Harmonic Loading with
Pitch-Flap Coupling, Rotor No. 4

The pitch-lag coupling effect is illustrated in Figure 31. A flap-lag instability occurs at a negative pitch-lag coupling of -0.6(-31°). While the slope of the curve was similar for Tail Rotor No. 1, sufficient lag damping was available. It appears that the large negative pitch-flap coupling of Tail Rotor No. 2 when combined with sufficient negative pitch-lag coupling will produce a flap-lag instability. Pitch-lag coupling had negligible effects on rotor loads. The destabilizing effects of θ_ζ and its coupling with θ_β are consistent with the predictions of Reference (25). It should be noted, however, that Reference (25) also shows that the effects of θ_ζ can be reversed. The following equation, derived from the results of Reference 26, shows the relationship between Z, θ_β, ω_ζ, p, β_0 and their effect on the destabilizing sense of θ_ζ:

$$\theta_\zeta \left[(\omega_\zeta^2 - p^2)(\frac{16\beta_0}{\gamma} + 2\bar{\phi} - \theta_0) - \frac{\gamma}{8}\bar{\phi}\theta_\beta - Z \right]$$

$$> 0 \quad \text{stabilizing}$$

$$< 0 \quad \text{destabilizing}$$

The above equation shows that θ_β or R can reverse the effect of θ_ζ. Equivalent negative values of R result when pre-elastic coupling is introduced, $Z = R(\theta_0 - \theta_{\text{pre-coupled}} + (\beta_0 - \beta_{pc})\theta_\beta)$ $(\omega_\zeta^2 - p^2 + 1)$
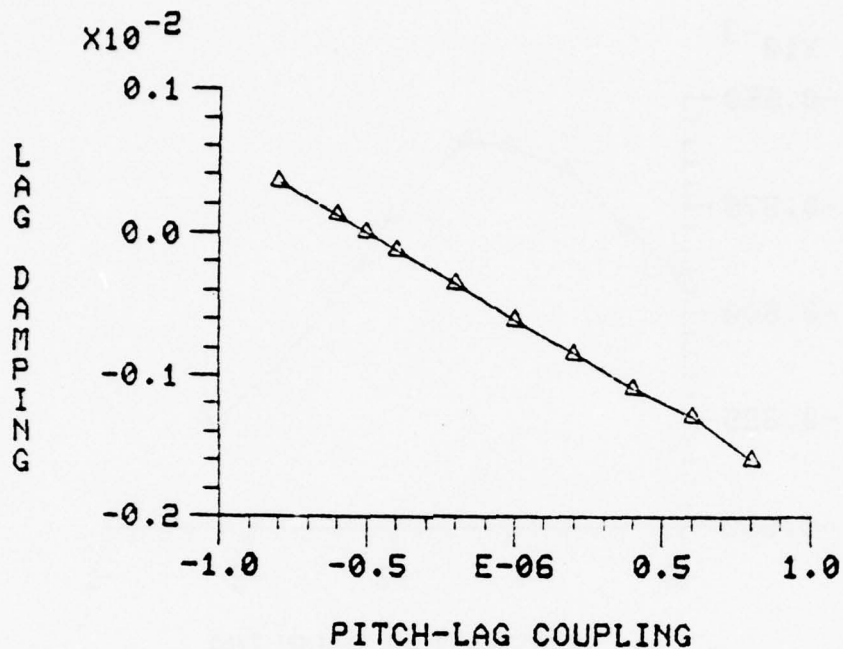
Figure 31. Variation of Lag Damping with Pitch-Lag Coupling, Rotor No. 4

Coalescence of the flap and lag frequencies at high col-lective pitch settings have been shown to cause flap-lag in-stabilities in References 22 and 24. While an instability did not occur at coalescence caused by the negative pitch-flap coupling sweep (Figure 27) a reduction in lag damping was evi-dent. This reduction is illustrated in Figure 32. Since the sweep was made at a moderate thrust setting, C_T = .0068, the rotor remained stable. To determine if the flap-lag instabil-ity of References 22 and 24 would occur a thrust variation was investigated at the value of pitch-lag coupling, θ_β = -3.5, which caused coalescence. The results are illustrated in Figure 33 and demonstrate a flap-lag instability at a thrust setting, C_T, of approximately .023.

$\times 10^{-3}$
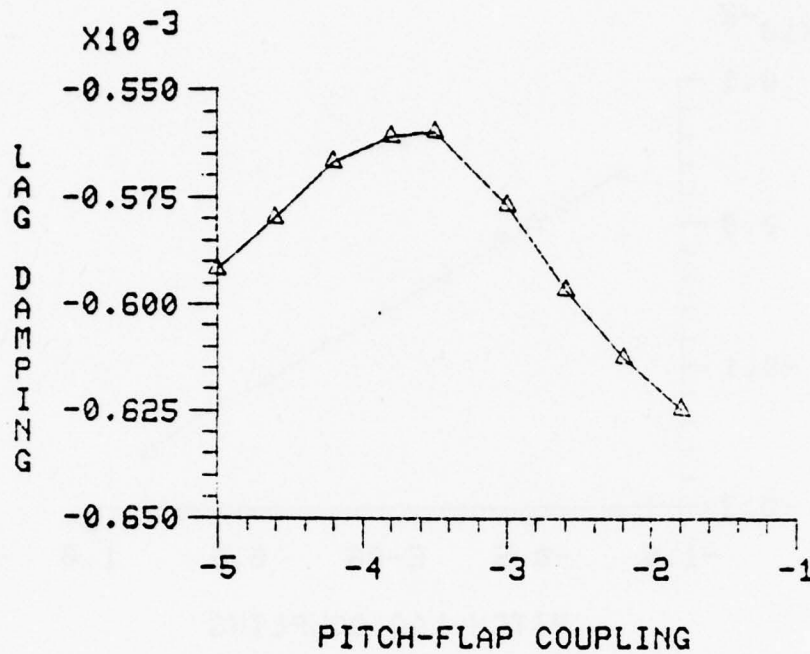
Figure 32. Variation of Lag Damping with Pitch-Flap Coupling, Rotor No. 4

$\times 10^{-3}$
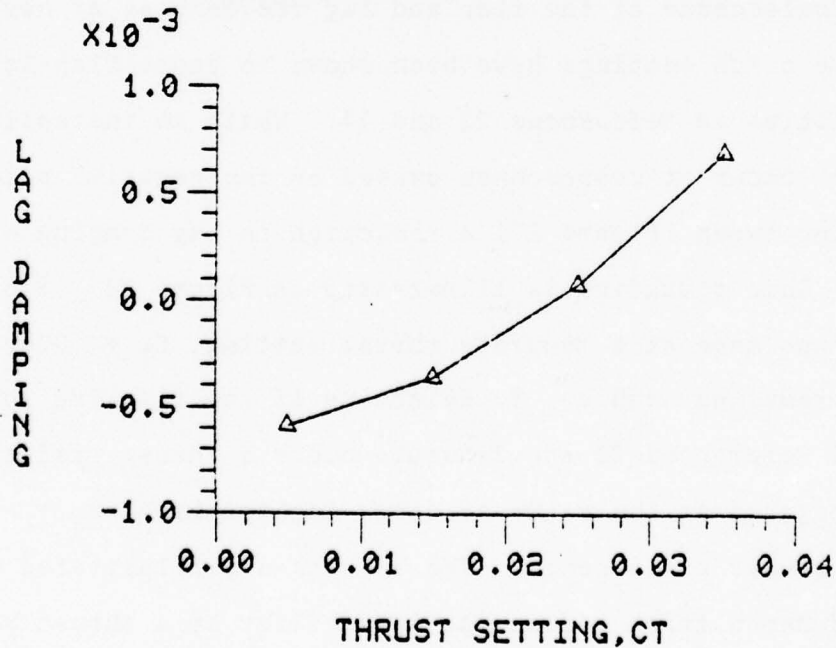
Figure 33. Variation of Lag Damping with Thrust Coefficient, Rotor No. 4

7. CONCLUSIONS AND RECOMMENDATIONS

7.1 CONCLUSIONS REGARDING THE METHOD

The method used to solve for blade stability and forced response is a modal decoupling analysis. First, the eigenvalues and periodic eigenfunctions are determined from Floquet theory. Second, the periodic eigenfunctions are used to uncouple the equations. The solution to the uncoupled equations is written by a simple harmonic balance, and the total solution is then obtained by superposition. The **following conclusions have been made based on extensive use** of the method:

(1) The fact that stability and vibrations are obtained from the identical set of equations allows direct comparison of the effects of parameters. Thus, the internal consistency insures that stability-forced response correlations are sound.

(2) The bookkeeping procedures that are required to keep track of the various modes and of their response require a significant initial investment in terms of computer programming and documentation. Once operational, however, the system runs very efficiently and requires 13 seconds per case on an IBM 360/65 computer.

(3) The initial programming has been done for the general case. Therefore, additional degrees of freedom or refinements to the mathematical model would require no substantial changes in the modal decoupling portion of the program.

(4) The results of the method allow quantitative evaluation of stability and vibrational characteristics without the tedious task of analyzing time histories.

7.2 CONCLUSIONS REGARDING EFFECT OF PARAMETERS

The results of the study show that the major rotor coupling parameters can be chosen in a systematic way to achieve both good stability and low vibrations in the rotating system. The following list indicates the manner in which the parameters could be chosen in a preliminary design:

(1) The first parameter to choose should be the elastic coupling, R. The results show that zero elastic coupling gives the smallest inplane loads. Although R also affects the damping, other parameters can be used to counter any destabilizing effects. Although R=0 is required at the most severe vibration condition, R may not necessarily equal zero for other operating conditions (and it may even become negative). This R range must be kept in mind when choosing the other parameters.

(2) The second parameter to be chosen is pitch-flap coupling, θ_3. This parameter should be given a large negative value in order to greatly reduce the 1/rev flapping loads in the rotating system for untrimmed rotors. For trimmed rotors, the 1/REV loads are approximately fixed by this trim setting, but negative θ_3 is still valuable for reducing the higher harmonic lag loads. Practical limits on negative θ_3 exist due to flying qualities and due to possible instability of higher modes, but θ_3 values as large as -2

to -3 are desirable from a vibration standpoint. Another
practical limitation on negative θ_β is the coalescence of
flap and lag frequencies at high collective pitch. The
results here **for moderate thrust produced no instabilities,**
for the case when negative θ_β causes a coalescence. At
higher collective pitch **or thrust coefficient setting,**
however, a coalescence or near coalescence did result in a
flap-lag instability. The importance of combined pitch-
flap and pitch-lag coupling is seen in the results here
in that the rotor with $\theta_\beta = -.7$ remains stable for θ_ζ as
large as -2.0, but the rotor with $\theta_\beta = -2.1$ becomes unstable
for $\theta_\zeta < -0.5$.

(3) The third parameter to be chosen is the pitch-lag
coupling, θ_ζ. Pitch-lag coupling has been shown to have
little effect on vibration but a large effect on stability.
Thus, once R and θ_β have been chosen so as to minimize
inplane and flapping loads, θ_ζ can be chosen to provide
stability without affecting the airloads. Reference 25
shows that θ_ζ should be chosen as positive for $\omega_\zeta > P$ and
as negative for $\omega_\zeta < P$. This is confirmed by the results
here. However, Reference 25 also shows that if R or θ_β
are significantly removed from zero, then the effect of θ_ζ
can be reduced or even reversed. Reference 13 shows a
similar reversal for soft inplane rotor at high advance
ratios. Therefore, care must be taken to analyze the
complete μ, R, θ_β range before choosing θ_ζ.

(4) The choice of precone and sweep in a blade design is not directly addressed in this work. Presumably, precone is chosen so as to eliminate the steady flap-bending moment. Precone and sweep have an important indirect effect on the stability and forced response which has been addressed here. That is, precone and sweep introduce virtual pitch-lag and pitch-flap couplings (26). Thus precone, sweep and virtual hinge sequence (flap-lag versus lag-flap) must be considered as sources of θ_ζ and θ_β in the blade design.

(5) The final parameter to be considered is the choice of viscous or elastomer lag dampers. The results here show that, although the lag damper improves stability, it also increases blade loads. Therefore, if sufficient θ_ζ is physically available, damping should be introduced by pitch-lag coupling rather than by dampers whenever possbile.

7.3 CONCLUSIONS REGARDING FUTURE WORK

The current research effort attains two separate goals. First, the research demonstrates the feasibility of using Floquet theory for forced response. Second, the research shows that the basic rotor couplings can be chosen in a logical manner to give both good stability and good vibrational characteristics. The work has also, however, raised new questions which should be studied as natural extensions of the present work.

1) The blade model should be improved to include higher modes in order that the effect of parameters on the high frequency vibrations can be determined. Present results

already indicate that θ_β may greatly reduce the higher harmonic inplane loads, but the effect of elasticity on these results is unknown.

2) Fuselage degrees of freedom should be added to the analysis. This would allow for a rational choice of fuselage and blade natural frequencies so as to lower vibrations.

3) Additional structural research should be performed so that any desired R, θ_β, θ_ζ combination could be designed into a rotor blade, including the option for fine-tuning these parameters after flight tests. (Some of this work **has already begun, References 27 and 28.**)

8. BIBLIOGRAPHY

1. Mil, M. L., et al., "Helicopter-Calculation and Design Vol. II, Vibrations and Dynamic Stability," NASA TT F-519, May 1968.

2. Schrage, D. P. and Peskar, R., "Helicopter Vibration Requirements," Proceedings, 33rd Annual National Forum of the American Helicopter Society, Washington, DC, May 1977.

3. Ormiston, R. A., "Comparison of Several Methods for Predicting Loads on a Hypothetical Helicopter Rotor," Journal of the American Helicopter Society, Vol. 19, No. 4, October 1974.

4. Blankenship, B. L. and Harvey, K. W., "A Digital Analysis for Helicopter Performance and Rotor Blade Bending Moments," Journal of the American Helicopter Society, Vol. 7, No. 4, October 1962.

5. Johnson, R.A., "Rotor Stability Prediction and Correlation with Model and Full-Scale Tests," Journal of the American Helicopter Society, Vol. 21, No. 2, April 1976.

6. Wood, E. R. and Hilizinger, K. D., "A Method for Determining the Fully Coupled Aeroelastic Response of Helicopter Rotor Blades," 19th Annual National Forum of the American Helicopter Society, May 1963.

7. Brandt, D. E., "Panel Discussion: Theoretical Analysis Versus Testing - A Trade Off," Proceedings from NASA Symposium on Flutter Testing, October 9-10, 1975.

8. Miao, W. L, et al., "Rotor Aeroelastic Stability Coupled with Helicopter Body Motion," Rotorocraft Dynamics, NASA-SP-352, February 1974.

9. Lange, B., "The Solution of Systems of Linear Differential Equations with Periodic Coefficients Applied to V/STOL Dynamic Analysis," Stanford University, Stanford, California.

10. Coddington, E. A. and Levinson, N., Theory of Ordinary Differential Equations, McGraw-Hill, New York 1955.

11. Brockett, R. W. , Finite Dimensional Linear Systems, John Wiley and Sons, New York, 1970.

12. Peters, D. A. and Hohenemser, K. H., "Application of the Floquet Transition Matrix to Problems of Lifting Rotor Stability," Journal of the American Helicopter Society, Vol. 16, No. 2, April 1971.

13. Peters, R. A., "Flap-Lag Stability of Helicopter Rotor Blades in Forward Flight," Journal of the American Helicopter Society, Vol. 20, No. 4, October 1975.

14. Hohenemser, K. H. and Yin, S. K., "Some Application of the Method of Multiblade Coordinates," Journal of the American Helicopter Society, Vol. 17, No. 3, July 1972.

15. Hammond, C. E., "An Application of Floquet Theory to Prediction of Mechanical Instability," Proceedings from AHS/NASA-Ames Specialists Meeeting on Rotorcraft Dynamics, Moffett Field, California, February 13-15, 1974.

16. Meirovitch, L., Elements of Vibration Analysis, McGraw-Hill, Inc., 1975.

17. Hodges, D. H. and Ormiston, R. A., "Nonlinear Equations for Bending of Rotating Beams with Application to Linear Flap-Lag Stability of Hingeless Rotors," NASA TM X-2770, May 1973.

18. Hodges, D. H. and Ormiston, R. A., "Stability of Elastic Bending and Torsion of Uniform Cantilever Rotor Blades in Hover with Variable Structural Coupling," NASA TN D-8192, April 1976.

19. Kaza, K.R.V. and Kvaternik, R. G., "A Critical Examination of the Flap-Lag Dynamics of Helicopter Rotor Blades in Hover and in Forward Flight," Proceedings, 32nd Annual National Forum of the American Helicopter Society, Washington, DC, May 1976.

20. Wei, F. S. and Peters, D. A., "Lag Damping in Auto-rotation by a Perturbation Method," Proceedings, 34th Annual National Forum of the American Helicopter Society, Washington, DC, May 1978.

21. Bramwell, A.R.S., Helicopter Dynamics, John Wiley and Sons, New York, 1976.

22. Edwards, W. T. and Miao, W., "Bearingless Tail Rotor Loads and Stability," USAAMRDL-TR-76-16, Applied Technology Laboratory, Research and Technology Laboratories (AVRADCOM) November 1977.

23. Fenaughty, R. R. and Noehren, W. L., "Composite Bearingless Tail Rotor for UTTAS," Journal of the American Helicopter Society, Vol. 22, No. 3, July 1977.

24. Ormiston, R. A. and Hodges, D. H., "Linear Flap-Lag Dynamics of Hingeless Helicopter Rotor Blades in Hover," Journal of the American Helicopter Society, Vol. 17, No. 2, April 1972.

25. Peters, D. A., "An Approximate Closed-Form Solution for Lead-Lag Damping of Rotor Blades in Hover," NASA TM X-62, 425, April 1975.

26. Peters, D. A. and Ormiston, R. A., "The Effects of Second Order Blade Bending on the Angle of Attach of Hingeless Rotor Blades," Journal of the American Helicopter Society, Vol. 18, No. 4, October 1973.

27. Ormiston, et al., "Hingeless Helicopter Rotor with Improved Stability," United States Patent 3,999,886, Dec. 28, 1976.

28. Bousman, W. G., Sharpe, D. L., and Ormiston, R. A., "An Experimental Study of Techniques for Increasing the Lead-Lag Damping of Soft Inplane Hingeless Rotors," Proceedings, 32nd Annual National Forum of the American Helicopter Society, Washington, DC, May 1976.

-71-

9.   APPENDICES

APPENDIX 9.1

Nomenclature

$[A(t)]$ - characteristic function matrix periodic with period T

BSHR,BMOM - nondimensional flap shear and flap moment, hub system

$[C(\psi)]$ - damping matrix, periodic with period T

C_{d_o} - blade profile drag coefficient

$\overline{C}_L, \overline{C}_M,$ - nondimensional roll, pitch, flap, and lag
$\overline{C}_{S\beta}, \overline{C}_{S\zeta}$ moments,
$$\frac{L,M,S}{\rho a c R^4 \Omega^2}$$

$\overline{C}_{V\beta}, \overline{C}_{V\zeta}$ - nondimensional flap and lag shears, $\dfrac{V}{\rho a c R^3 \Omega^2}$

C_{VH} - nondimensional lag shear, hub coordinates

C_T - thrust coefficient, $\dfrac{T}{\rho(\Omega R)^2 \pi R^2}$

$[D(t)]$ - matrix of periodic equation coefficients

DPL - lag damper setting, per cent critical damping

F - fixed system

F_β, F_ζ - force per unit length, perpendicular to blade and also perpendicular and parallel, respectively, to direction of rotation:
$$\overline{F}_\beta = R^2 F_\beta / \Omega^2 I, \quad \overline{F}_\zeta = R^2 F_\zeta / \Omega^2 I$$

I - blade inertia or identity matrix

I_β - flap moment of inertia

ISP - sweep identification parameter

$[K(\psi)]$ - stiffness matrix, periodic with period T

$K_{\beta\beta}$ - flap stiffness

$K_{\beta\zeta}$ - flap-lag cross stiffness

$K_{\zeta\zeta}$ - lag stiffness

KY - trim identification parameter

L - roll moment for one blade (right side down)

$[L(\psi)]$ - forcing coefficient matrix

M - pitch moment for one blade (nose-up)

$[M(\psi)]$ - forcing coefficient matrix

$[N(\psi)]$ - forcing coefficient matrix

NSP - sweep or no sweep identification parameter

$[O(\psi)]$ - forcing coefficient matrix

O( ) - order of

P - stiffness parameter

Q - Floquet Transition Matrix (FTM)

R - blade radius or elastic coupling parameter

RFL - hinge sequence identification parameter

RT - pitch bearing sequence identification parameter

T - rotor thrust or period of one revolution, $T=2\pi/\Omega$

U - total velocity of blade section relative to air

U_P, U_T - local velocity of blade relative to air in F_β and F_ζ directions, respectively

$\overline{U}_P, \overline{U}_T$ - nondimensional velocities $U_P/\Omega R$, $U_T/\Omega R$

V_i - uniform induced velocity in negative z direction

V_x, V_z - components of helicopter speed in negative x and z directions, respectively

W - stiffness parameter

X,Y,Z - aircraft coordinates

Z - stiffness parameter

ZSC - lag shear correction factor

ZSHR,ZMOM - nondimensional lag shear and lag moment

a - lift curve slope

a_n - Fourier coefficients for $g(t)$

b - number of blades

c - blade chord

d - local blade drag per unit length

e - hinge offset

$f(t)$ - periodic forcing function in coupled equations

$g(t)$ - periodic forcing function in uncoupled equations

i - $\sqrt{-1}$

ℓ - local blade lift per unit length

n - harmonic number

p - dimensionless rotating flap frequency at $\bar{\theta} = 0$
$$p = \sqrt{P}(\theta - 0) = \sqrt{1 + \omega_\beta^2}$$

q - generalized coordinate

r - blade radial coordinate

$\bar{r}$ - nondimensional coordinate, r/R

t - time

$\bar{t}$ - nondimensional time = $\psi = \Omega t$

$\bar{x}$ - nondimensional longitudinal shear

$x(t)$ - state vector, coupled response

x,y,z - rotating blade coordinates

$\bar{y}$ - nondimensional lateral shear

$y(t)$ - state vector, uncoupled response

α - constants determined from initial conditions

β - flap angle, positive up

$\overline{\beta}$ - equilibrium flapping angle, $\beta_o + \beta_s s\psi + \beta_c c\psi$

β_o - coning angle

β_s - lateral cyclic flap angle

β_c - longitudinal cyclic flap angle

β_{pc} - pre-cone angle

γ - Lock number, $\rho a c R^4 / I$

$\delta\beta, \delta\zeta$ - perturbation flap and lag angles

ϵ - small quantity

ϵ_β - small flap angle quantity

ζ - lag angle, positive forward

$\overline{\zeta}$ - equilibrium lag angle

η - real portion of lag eigenvalue

θ - pitch angle, $\overline{\theta} + \theta_\beta \delta\beta + \theta_\zeta \delta\zeta$

$\overline{\theta}$ - equilibrium pitch angle, $\theta_o + \theta_s s\psi + \theta_c c\psi$
$+ \theta_\beta(\overline{\beta} - \beta_{pc}) + \theta_\zeta \overline{\zeta}$

θ_o - collective pitch angle

θ_s - longitudinal cyclic pitch angle

θ_c - lateral cyclic pitch angle

$\theta_\beta, \theta_\zeta$ - pitch-flap and pitch-lag coupling ratios

Λ - complex eigenvalue, $\Lambda = \eta + i\omega$

λ - inflow ratio, $(V_i + V_z)/\Omega R$

μ - advance ratio, $V_x/\Omega R$

ρ - density of air

σ - rotor solidity, $bc/\pi R$

$\phi(t)$ - state transition matrix

$\overline{\phi}$ - inflow parameter, $\overline{\phi} = 4/3\lambda$

ψ - rotor azimuth angle, $\psi = 0$ aft, $\psi = \Omega r$, dimensionless time

Ω - rotor angular velocity

ω - imaginary portion lag eigenvalue

$\omega_\beta, \omega_\zeta$ - dimensionless nonrotating flap and lag frequencies at $\theta = 0$

$s\psi, c\psi$ - $\sin(\psi)$, $\cos(\psi)$

[ ] - square matrix

{ } - column vector

< > - row vector

$(\cdot)$ - $\frac{d}{d\psi}(\ ) = \frac{1}{\Omega}\frac{d}{dt}(\ )$

$^{-}$ - nondimensional

$\rightarrow$ - vector

APPENDIX 9.2

Derivation of Flap-Lag Equations, Shears, and Moments

9.2.1 Derivation of Flap-Lag Equations

Considering the centrally hinged, spring restrained, rigid blade representation in Figure 3 the nonlinear flap-lag equations can be obtained from Lagrange's Equations:

$$\frac{d}{dt}\left(\frac{\partial T}{\partial \dot{q}}\right) - \frac{\partial T}{\partial q} + \frac{\partial V}{\partial q} = f$$

where

$$T = \frac{1}{2}I\cos^2\beta(\Omega+\dot{\zeta})^2 + \frac{1}{2}I(\dot{\beta})^2 \qquad \text{(Kinetic Energy)}$$

$$V = \frac{1}{2}K_{\beta\beta}\beta^2 + \frac{1}{2}K_{\zeta\zeta}\zeta^2 + K_{\beta\zeta}\beta\zeta \qquad \text{(Potential Energy)}$$

$$W = \int_0^R \left[F_\zeta(r)r\cos\beta\delta\zeta + F_\beta(r)r\delta\beta\right] dr \qquad \text{(Virtual Work)}$$

These expressions can be differentiated with respect to β, $\dot{\beta}$, ζ and $\dot{\zeta}$ to obtain the nonlinear flap-lag equations of motion of Reference 13:

$$\ddot{\beta} + \sin\beta\cos\beta(1+\dot{\zeta})^2 + (P-1)(\beta-\beta_{pc}) + Z\zeta = \int_0^1 \overline{F}_\beta \overline{r}d\overline{r} = f_\beta$$

$$\tag{9.2.1}$$

$$\cos^2\beta\ddot{\zeta} - 2\sin\beta\cos\beta(1+\dot{\zeta})\dot{\beta} + W\zeta + Z(\beta-\beta_{pc}) = \cos\beta\int_0^1 \overline{F}_\zeta \overline{r}d\overline{r} = f_\zeta$$

(where time has been made nondimensional, i.e. $\overline{t} = \psi = \Omega t$). The elastic terms are approximated, assuming small pitch angle, as:

$$P = 1 + \omega_\beta^2 = p^2 \; ; \; W = \omega_\zeta^2 \; ; \; Z = R(\omega_\zeta^2 - \omega_\beta^2)\theta$$

The nondimensional airloads, $\overline{F}_\beta$ and $\overline{F}_\zeta$, are illustrated at a blade element in Figure 9.2.1.
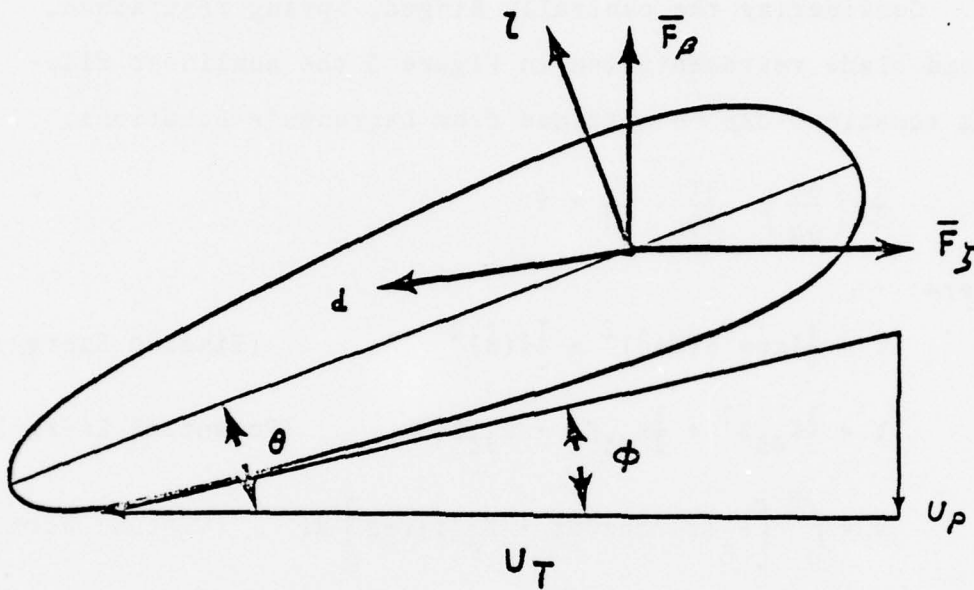
Figure 9.2.1.   Blade Element Geometry

The element aerodynamic forces $\overline{F}_\beta$ and $\overline{F}_\zeta$ are obtained from quasi-steady airfoil (blade element or strip) theory. Therefore, summation of forces in the β and ζ directions yield:

$$\overline{F}_\beta = \ell\cos\phi - d\sin\phi$$
$$\overline{F}_\zeta = -d\cos\phi - \ell\sin\phi \qquad\qquad (9.2.2)$$

From Figure 9.2.1: $\phi = \tan^{-1}(U_p/U_T)$, $U = (U_p^2 + U_T^2)^{1/2}$

From the fundamentals of aerodynamics the lift and drag per unit length are:

$$\ell = \frac{\rho a c}{2} U^2 \sin(\theta-\phi), \, d = \frac{\rho a c}{2} U^2 \frac{C_{d_o}}{a}$$

The nondimensional force components $\overline{F}_\beta$ and $\overline{F}_\zeta$ are obtained from Equation (9.2.2) as:

$$\overline{F}_\beta = \frac{\gamma}{2} \, \overline{U}_T^2 \sin\theta - \overline{U}_T \overline{U}_p (\cos\theta + \frac{C_{d_o}}{a})$$

$$\overline{F}_\zeta = \frac{\gamma}{2} \, \overline{U}_p^2 (\cos\theta - \frac{1}{2} \frac{C_{d_o}}{a}) - \overline{U}_p \overline{U}_T \sin\theta - \overline{U}_T^2 \frac{C_{d_o}}{a}$$

(9.2.3)

The nondimensional velocities $\overline{U}_T$ and $\overline{U}_p$ are:

$$\overline{U}_T = (1+\dot{\zeta})\overline{r}\cos\beta + \mu\sin(\psi+\zeta)$$

(9.2.4)

$$\overline{U}_p = \overline{r}\dot{\beta} + \lambda\cos\beta + \mu\sin\beta\cos(\psi+\zeta)$$

To obtain linear free vibration equations, small perturbation motions about a periodic equilibrium motion of the nonlinear system are considered. The equilibrium values of θ, ζ, and β are designated $\overline{\theta}(\psi)$, $\overline{\zeta}(\psi)$, and $\overline{\beta}(\psi)$. These form the basis of the perturbation expansions:

$$\zeta = \overline{\zeta} + \delta\zeta, \, \beta = \overline{\beta} + \delta\beta, \, \theta = \overline{\theta} + \theta_\beta\delta\beta + \theta_\zeta\delta\zeta \quad (9.2.5)$$

where θ_β and θ_ζ are pitch-flap and pitch-lag coupling parameters. Positive θ_β and θ_ζ implies that the blade pitches up due to positive flapping or lead inplane motions. The perturbation equations are obtained by substitution of Equation (9.2.5) into the Equation (9.2.1), cancellation of the appropriate equilibrium terms, collection of linear terms in $\delta\zeta$ and $\delta\beta$ on the

left-hand side (LHS), collection of the remaining nonlinear terms on the right-hand side (RHS), and neglect of the higher order quantities $\overline{\zeta}$, $\dot{\overline{\zeta}}$, $\overline{\beta}^2$, $\beta\dot{\overline{\beta}}$, and $\dot{\overline{\beta}}^2$ with respect to unity in the $\delta\zeta$ and $\delta\beta$ coefficients. By neglect of reversed flow and use of the fact that C_{d_o} is small with respect to unity, the following flap-lag forced response and stability equations are obtained:

$$
\left\{ \begin{matrix} \circ\ddot{\beta} \\ \delta\ddot{\zeta} \end{matrix} \right\} + \left[C(\psi) \right] \left\{ \begin{matrix} \delta\dot{\beta} \\ \delta\dot{\zeta} \end{matrix} \right\} + \left[K(\psi) \right] \left\{ \begin{matrix} \delta\beta \\ \delta\zeta \end{matrix} \right\} =
$$

$$
\left[L(\psi) \right] \left\{ \begin{matrix} \dot{\overline{\beta}} \\ \overline{\beta} \end{matrix} \right\} + \left[M(\psi) \right] \left\{ \begin{matrix} \overline{\theta} \\ \overline{\phi} \end{matrix} \right\} + \left[N(\psi) \right] \left\{ \begin{matrix} \ddot{\overline{\beta}} \\ C_{d_o}/a \end{matrix} \right\}
$$

$$
+ \left\{ 0(\psi) \right\} \beta_{pc}
$$

where

$$
C(\psi) = \left[\begin{matrix} \frac{\gamma}{8}(1+\frac{4}{3}\mu s\psi) & \begin{array}{l} \frac{\gamma}{8}(\overline{\phi}+\frac{4}{3}\mu c\psi\overline{\beta}+\dot{\overline{\beta}}) \\[4pt] -2\frac{\gamma}{8}\overline{\theta}(1+\frac{4}{3}\mu s\psi) + 2\overline{\beta} \end{array} \\[20pt] \begin{array}{l} -2\frac{\gamma}{8}(\overline{\phi}+\frac{4}{3}\mu c\psi\overline{\beta}+\dot{\overline{\beta}}) \\[4pt] +\frac{\gamma}{8}\overline{\theta}(1+\frac{4}{3}\mu s\psi)-2\overline{\beta} \end{array} & \begin{array}{l} \frac{\gamma}{8}\overline{\theta}(\overline{\phi}+\frac{4}{3}\mu c\psi\ \overline{\beta}+\dot{\overline{\beta}})-2\overline{\beta}\ \dot{\overline{\beta}} \\[4pt] + 2\ \dfrac{C_{d_o}}{a}\ \frac{\gamma}{8}(1+\frac{4}{3}\mu s\psi) + 2(DPL)\omega_\zeta \end{array} \end{matrix} \right]
$$

$$K(\psi) = \begin{bmatrix} \begin{array}{l} P \\[6pt] + \dfrac{\gamma}{8}\left(\dfrac{4}{3}\mu c\psi + 2\mu^2 s\psi c\psi\right) \\[6pt] - \dfrac{\gamma}{8}\theta_\beta\left(1 + \dfrac{8}{3}\mu s\psi + 2\mu^2 s^2\psi\right) \end{array} & \begin{array}{l} Z + \dfrac{\gamma}{8}\mu c\psi\left(\dfrac{3}{2}\overline{\phi} + \dfrac{4}{3}\dot{\overline{\beta}}\right) \\[6pt] - 2\dfrac{\gamma}{8}\overline{\theta}\left(\dfrac{4}{3}\mu c\psi + 2\mu^2 s\psi c\psi\right) \\[6pt] + 2\dfrac{\gamma}{8}\overline{\beta}\left(\mu^2 c^2\psi - \mu^2 s^2\psi - \dfrac{2}{3}\mu s\psi\right) \\[6pt] - \dfrac{\gamma}{8}\theta_\zeta\left(1 + \dfrac{8}{3}\mu s\psi + 2\mu^2 s^2\psi\right) \\[6pt] + RFL\ \dfrac{\gamma}{8}\left(1 + \dfrac{8}{3}\mu s\psi + 2\mu^2 s^2\psi\right)\overline{\beta} \end{array} \\ \hline \begin{array}{l} Z - 2\dot{\overline{\beta}} - 2\dfrac{\gamma}{8}\mu c\psi\left(\dfrac{3}{2}\overline{\phi} + \dfrac{4}{3}\dot{\overline{\beta}}\right) \\[6pt] + \dfrac{\gamma}{8}\overline{\theta}\left(\dfrac{4}{3}\mu c\psi + 2\mu^2 s\psi c\psi\right) \\[6pt] - 4\dfrac{\gamma}{8}\overline{\beta}\mu^2 c^2\psi + R\theta_\beta(\overline{\beta} - \beta_{pc}) \\[6pt] \quad (\omega_\zeta^2 - \omega_\beta^2) \\[6pt] + \dfrac{\gamma}{8}\theta_\beta\left[\overline{\phi}\left(1 + \dfrac{3}{2}\mu s\psi\right) + \dot{\overline{\beta}}\left(1 + \dfrac{4}{3}\mu s\psi\right)\right. \\[6pt] \left. + \overline{\beta}\left(\dfrac{4}{3}\mu c\psi + 2\mu^2 s\psi c\psi\right)\right] \end{array} & \begin{array}{l} W + \dfrac{\gamma}{8}\left[2\dfrac{C_{d_o}}{a}\left(\dfrac{4}{3}\mu c\psi + 2\mu^2 s\psi c\psi\right)\right. \\[6pt] + \mu c\psi\overline{\theta} \\[6pt] \times\left(\dfrac{3}{2}\overline{\phi} + \dfrac{4}{3}\dot{\overline{\beta}}\right) - \overline{\beta}\ \ \overline{\theta}\left(\dfrac{4}{3}\mu s\psi + 2\mu^2 s^2\psi\right. \\[6pt] \left. - 2\mu^2 c^2\psi\right) \\[6pt] \left. + 2\mu s\psi\overline{\beta}\left(\dfrac{3}{2}\overline{\phi} + \dfrac{4}{3}\dot{\overline{\beta}} + 2\mu c\psi\overline{\beta}\right)\right] \\[6pt] + \dfrac{\gamma}{8}\theta_\zeta\left[\overline{\phi}\left(1 + \dfrac{3}{2}\mu s\psi\right)\right. \\[6pt] + \overline{\beta}\left(\dfrac{4}{3}\mu c\psi + 2\mu^2 s\psi c\psi\right) \\[6pt] \left. + \dot{\overline{\beta}}\left(1 + \dfrac{4}{3}\mu s\psi\right)\right] \\[6pt] + RFL\dfrac{\gamma}{8}\left(1 + \dfrac{8}{3}\mu s\psi + 2\mu^2 s^2\psi\right)\overline{\beta}\ \ \overline{\theta} \\[6pt] - RFL\ \dfrac{\gamma}{8}\left(3\overline{\phi}\mu s\psi + \dfrac{8}{3}\dot{\overline{\beta}}\mu s\psi\right. \\[6pt] \left. - 4\mu^2 s\psi c\psi\right)\ \overline{\beta} \\[6pt] - RFL\ \dfrac{\gamma}{8}\left(2\overline{\phi} + 2\dot{\overline{\beta}} + \dfrac{8}{3}\mu c\psi\overline{\beta}\right)\ \ \overline{\beta} \end{array} \end{bmatrix}$$

$$L(\psi) = \left[\begin{array}{c|c} -\dfrac{\gamma}{8}(1+\dfrac{4}{3}\mu s\psi) & \begin{array}{c} -p \\ -\dfrac{\gamma}{8}(\dfrac{4}{3}\mu c\psi+2\mu^2 s\psi c\psi) \end{array} \\ \hline \begin{array}{c} \dfrac{\gamma}{8}(2\bar{\phi}+\dfrac{8}{3}\bar{\beta}\mu c\psi+\dot{\bar{\beta}}) \\ -\dfrac{\gamma}{8}\bar{\theta}(1+\dfrac{4}{3}\mu s\psi)+2\bar{\beta} \end{array} & \begin{array}{c} \dfrac{\gamma}{8}(3\bar{\phi}\mu c\psi+2\mu^2 c^2\psi\bar{\beta}) \\ -\dfrac{\gamma}{8}\bar{\theta}(\dfrac{4}{3}\mu c\psi+2\mu^2 c\psi s\psi) \\ -Z-R(\omega_\zeta^2-\omega_\beta^2)\theta_\beta \end{array} \end{array}\right] \qquad O(\psi) = \left\{\begin{array}{c} P-1 \\ \hline RT\ddot{\theta}+Z \\ +R(\omega_\zeta^2-\omega_\beta^2)\theta_\beta \end{array}\right\}$$

$$M(\psi) = \left[\begin{array}{c|c} \dfrac{\gamma}{8}(1+\dfrac{8}{3}\mu s\psi+2\mu^2 s^2\psi) & -\dfrac{\gamma}{8}(1+\dfrac{3}{2}\mu s\psi) \\ \hline -\dfrac{\gamma}{8}\bar{\phi}(1+\dfrac{3}{2}\mu s\psi) & \dfrac{\gamma}{8}(\dfrac{9}{8}\bar{\phi}) \end{array}\right] \qquad N(\psi) = \left[\begin{array}{c|c} -1 & 0 \\ \hline 0 & \begin{array}{l} -\dfrac{\gamma}{8}(1+ \\ \dfrac{8}{3}\mu s\psi+ \\ 2\mu^2 s^2\psi) \end{array} \end{array}\right]$$

9.2.2 Derivation of Flap-Lag Shears and Moments

The absolute (inertial) acceleration of a particle whose position is expressed relative to a rotating frame is expressed as (Reference 21):

$$\vec{a} = \frac{\partial^2 \vec{r}}{\partial t^2} + \vec{\Omega} \times (\vec{\Omega}\times\vec{r}) + 2\vec{\Omega} \times \frac{\partial \vec{r}}{\partial t} + \frac{\partial \vec{\Omega}}{\partial t} \times \vec{r} \qquad (9.2.6)$$

We now apply Equation 9.2.6 to calculate the acceleration of an element of the moving rotor blade of Figure 3. The radius vector of a point P on the blade can be written as:

$$\vec{r} = r\cos\beta\vec{i} + r\sin\beta\vec{k}$$

$$\vec{\Omega} = (\Omega+\zeta)\vec{k} \quad \text{(angular velocity)}$$

where a set of unit vectors $\vec{i}$, $\vec{j}$, and $\vec{k}$ have been defined such that $\vec{k}$ lies along the shaft and $\vec{i}$ lies in the flapping plane. Unit vector $\vec{j}$ is defined by taking the right hand rule. Performing the vector and partial differentiation operations of Equation (9.2.1) the acceleration of the point P is obtained:

$$\vec{a} = -r(\Omega^2 + 2\Omega\dot{\zeta} + \dot{\beta}^2 + \beta\ddot{\beta})\vec{i} + r(\ddot{\zeta} - 2\Omega\dot{\beta}\beta)\vec{j} + r\ddot{\beta}\vec{k}$$

The acceleration in each direction combined with flap and lag aerodynamic loadings can be used to calculate the hub shears and moments.

9.2.2.1 Rotating System Hub Shears

The hub shears in the rotating system can be resolved into $\bar{C}_{V\beta}$, $\bar{C}_{V\zeta}$, and $\bar{C}_{VR}$ which are illustrated in Figure 9.2.2. The shears are expressed as integrals of the blade aerodynamic and inertial loadings.
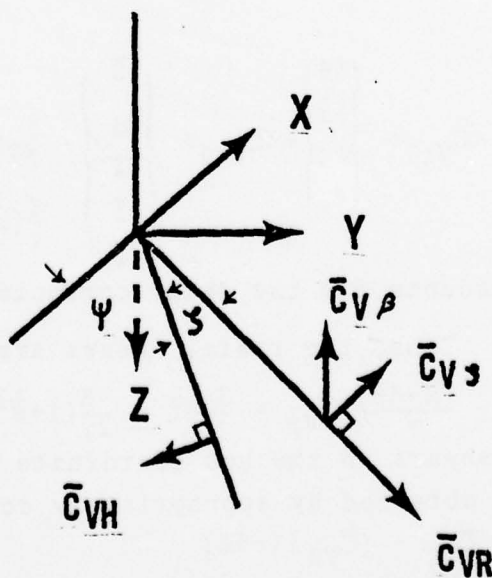
Figure 9.2.2. Rotating Hub Shear Components

The flap shears, $\overline{C}_{V\beta}$, are:

$$\overline{C}_{V\beta} = \frac{1}{\gamma} \int_0^1 F_\beta \, d\overline{r} - \frac{3}{2\gamma} \ddot{\beta}$$

Substituting the expression for $\overline{F}_\beta$ and integrating yields:

$$\overline{C}_{V\beta} = \langle \overline{C}_{V\beta 1} \rangle \begin{Bmatrix} \delta\beta \\ \delta\dot{\beta} \\ \delta\zeta \\ \delta\dot{\zeta} \end{Bmatrix} + \langle \overline{C}_{V\beta 2} \rangle \begin{Bmatrix} \overline{\beta} \\ \dot{\overline{\beta}} \\ \overline{\theta} \\ \overline{\phi} \end{Bmatrix} - \frac{3}{2\gamma}(\ddot{\overline{\beta}} + \delta\ddot{\beta})$$

The coefficients $\overline{C}_{V\beta 1}$ and $\overline{C}_{V\beta 2}$ contain similar periodic terms found in the flap-lag equations. The numerical coefficients of the terms will be different, however, since there is an extra $\overline{r}$ in the aerodynamic forcing term expressions on the right hand side of the nonlinear flap-lag equations (Equation 9.2.1).

The lag shears are obtained in a similar manner.

$$\overline{C}_{V\zeta} = \frac{1}{\gamma} \int_0^1 \overline{F}_\zeta \, d\overline{r} - \frac{3}{2\gamma}\ddot{\zeta} + \frac{3}{\gamma}\beta\dot{\beta}$$

which becomes:

$$\overline{C}_{V\zeta} = \langle \overline{C}_{V\zeta 1} \rangle \begin{Bmatrix} \delta\beta \\ \delta\dot{\beta} \\ \delta\zeta \\ \delta\dot{\zeta} \end{Bmatrix} + \langle \overline{C}_{V\zeta 2} \rangle \begin{Bmatrix} \overline{\beta} \\ \dfrac{C_{d_o}}{a} \\ \overline{\theta} \\ \overline{\phi} \end{Bmatrix} - \frac{3}{2\gamma}\delta\ddot{\zeta} + \frac{3}{\gamma}(\dot{\overline{\beta}}\overline{\beta} + \dot{\overline{\beta}}\delta\beta + \overline{\beta}\delta\dot{\beta}) - \frac{2}{\gamma}(DPL)(ZSC)\omega_\zeta\delta\dot{\zeta}$$

(where ZSC accounts for the shear correction between damper attachments). Thus, the radial shears are:

$$\overline{C}_{VR} = -\frac{(\overline{\beta}+\delta\beta)}{\gamma}\,\overline{C}_{V\beta} + \frac{3}{\gamma}\delta\dot{\zeta} + \frac{3}{2\gamma}(1 + \dot{\overline{\beta}}^2 + 2\dot{\overline{\beta}}\delta\dot{\beta} - \overline{\beta}^2/2 - \overline{\beta}\delta\beta)$$

The lag shears in the hub coordinate system, $\overline{C}_{VH}$ (Figure 9.2.2), can be obtained by appropriately combining $\overline{C}_{V\zeta}$ and $\overline{C}_{VR}$:

$$\overline{C}_{VH} = -\overline{C}_{V\zeta} + (\overline{C}_{VR})(-\delta\zeta)$$

These are the horizontal and lag shears used in the thesis.

9.2.2.2 Fixed System Hub Shears

The fixed system shears can be obtained from the rotating shears utilizing the coordinate system in Figure 9.2.3.
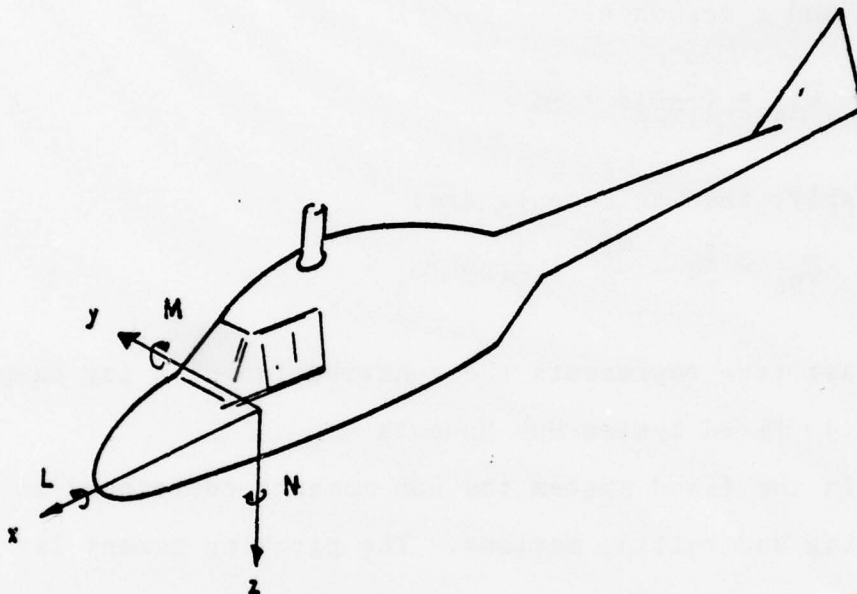
Figure 9.2.3. Fixed System Coordinates

In the forward, x, direction:

$$\overline{x} = \overline{C}_{V\zeta}\sin\psi + (\overline{C}_{V\beta}\cos\psi)(\overline{\beta}+\delta\beta) - \frac{3}{\gamma}\delta\dot{\zeta}\cos\psi$$

$$- \frac{3}{2\gamma}(\dot{\overline{\beta}}^2+2\dot{\overline{\beta}}\delta\dot{\beta})\cos\psi + \frac{3}{2\gamma}\delta\zeta\sin\psi + \frac{3}{2\gamma}(\overline{\beta}^2+2\overline{\beta}\delta\beta)\frac{1}{2}\cos\psi$$

In the lateral, y, direction:

$$\overline{y} = \overline{C}_{V\zeta}\cos\psi - (\overline{C}_{V\beta}\sin\psi)(\overline{\beta}+\delta\beta) + \frac{3}{\gamma}\delta\dot{\zeta}\sin\psi$$

$$+ \frac{3}{2\gamma}(\dot{\overline{\beta}}^2+2\dot{\overline{\beta}}\delta\dot{\beta})\sin\psi + \frac{3}{2\gamma}\delta\zeta\cos\psi - \frac{3}{2\gamma}(\overline{\beta}^2+2\overline{\beta}\delta\beta)\frac{1}{2}\sin\psi$$

In the vertical, z, direction:

$$\bar{z} = - \bar{C}_{V\beta}$$

9.2.2.3 Rotating System Hub Moments

The flap moments are obtained almost directly from the β and ζ responses:

$$\bar{C}_{S\beta} = (\frac{P-1}{\gamma})\beta + \frac{Z}{\gamma}\zeta$$

Similarly, the lag moments are:

$$\bar{C}_{S\zeta} = \frac{Z}{\gamma}\beta + \frac{\omega_{\zeta}^2}{\gamma}\zeta + \frac{2}{\gamma}(DPL)\omega_{\zeta}\dot{\zeta}$$

The last term represents the contribution of a lag damper.

9.2.2.4 Fixed System Hub Moments

In the fixed system the hub moments correspond to pitching and rolling motions. The pitching moment is:

$$\bar{C}_M = - \bar{C}_{S\beta}\cos(\psi)$$

The rolling moment is:

$$\bar{C}_L = - \bar{C}_{S\beta}\sin(\psi)$$

The sign conventions are illustrated in Figure 9.2.3.

-87-

APPENDIX 9.3

Computer Programs

9.3.1 Main Program Listing

```
C------------------------------------------------------------        00000020
C FLAP-LAG FORWARD FLIGHT-FORCED RESPONSE AND STABILITY  -           0000003C
C                 MAIN PROGRAM                           -           0000004C
C------------------------------------------------------------        00000050
C                                                                    0C000060
      DIMENSION PRMT(5),DERY(20),Y(20),AUX(16,20),D(20,20),RSST(20,2), 00000070
     1AS(1040),ETA(6),DUMR(4,4),DUMI(4,4),DUMRV(16),DUMIV(16),        00000080
     2GTR(6),GTI(6),GRT(390),GIT(390),GFT(12),YTR(65),YTI(65)         00000090
      DIMENSION YR(390),YI(390),YT(390),DUMA(20),DUMY(6),XT(6),XTR(6), 00000100
     1XTI(6),XRT(390),XIT(390)                                        00000110
      DIMENSION F(20),FM(6),FT(6)                                     0000012C
      DIMENSION LWL(6),MWM(6)                                         00000130
      DIMENSION FXT(65),XFA(50),A(12),B(12)                           00000140
      DIMENSION FYR(65),FYI(65),YRFA(50),YIFA(50)                     00000150
      DIMENSION RBSHR(65),RZSHR(65)                                   0C000160
      DIMENSION FXBT(65),XFBA(50)                                     00C00161
      DOUBLE PRECISION DUVR,DUVI                                      0C000170
      DOUBLE PRECISION DUMR,DUMI                                      0C0C018C
      DOUBLE PRECISION D,RSST                                         00030190
      COMPLEX QP,QN,QCT,QST,GFT,SYT,YCP,YCN                           00000200
      COMPLEX AS,DUMV,CP,CN,CTF,YT,DUMA,DUMY,ETA,XT                   0C0C0210
      COMPLEX CDUM,AVG                                                00000220
      COMMON/S/KZ                                                     00000230
      COMMON/Q/PHI(1040)                                             03000240
      COMMON/SA/AS                                                    00000250
      COMMON/INT/NC,MR,NS,NS2,IN,NH,NR                                00000260
      COMMON/STR/P,WZ,R,W,Z,PHIB,RW,DPL                               0C000270
      COMMON/GEM/RFL,RT,ZSC                                           00000280
      COMMON/ST2/WB2,WZ2,CT,ST                                        00000290
      COMMON/PAR/U,GAM,SD,CTC,GAMB                                    00000300
      COMMON/GEQ/BZ,THS,THC,SIG,CPB,CPL,BC,BS,BC,THZ                  0000031C
      COMMON/FOUR/AL(12),BL(12),AB(12),BB(12),FNT(65),GNT(65)         00000320
      COMMON/FS/THF                                                   00000321
      EXTERNAL FCT,OUTP,MATZ                                          0000033C
C                                                                    00000340
  100 FORMAT(1H1,25H FLAP-LAG FORCED RESPONSE)                        00000350
  200 FORMAT(6F10.6)                                                  00000360
  201 FORMAT(15I5)                                                    0G000370
  600 FORMAT(5X,9F10.6)                                               0C000380
  601 FORMAT(5X,12(I5,5X))                                            00000390
  602 FORMAT(6X,8E10.3)                                               00000400
    1 FORMAT(7X,3H NO,7X,3H MR,7X,3H NS,7X,3H NH,7X,3H IN,7X,3H NR,7X, 0C00041C
     13HISP,7X,3HNSP,7X,3H KY)                                        0GC00420
    2 FORMAT(7X,3H P ,7X,3H WZ,7X,3H R ,7X,3HRFL,7X,3H RT,7X,3HDPL)    00000430
    3 FORMAT(7X,3H U ,7X,3HGAM,7X,3H SD,7X,3HCTC,7X,3HSIG,7X,3H AA)    0000044C
    4 FORMAT(7X,3H BZ,7X,3HTHS,7X,3HT-C,7X,3HCPF,7X,3HCPL,7X,3HZSC)    00000450
    5 FORMAT(7X,3H BC,7X,3H BS,7X,3H BC,7X,3HTHZ,7X,4HPHIB,7X,4HPHIH,  00000460
     17X,3HTHF)                                                       00000461
C INPUT PARAMETERS FOR THIS CASE                                     00000470
C                                                                    00000480
C                                                                    00000490
      READ(5,201) NO,MR,NS,NH,IN,NR,ISP,NSP,KY                        00000500
      READ(5,200) P,WZ,R,RFL,RT,DPL                                   0000051C
      READ(5,200) U,GAM,SD,CTC,SIG,AA                                 0000052C
      READ(5,200) BZ,THS,THC,THZ,CPB,CPL,ZSC                          00000530
      READ(5,200) BC,BS,BC,PHIB,PHIH,THF                             00000540
      SD=SD/AA                                                        00000541
C                                                                    0C000550
C                                                                    00000560
C INITIALIZE PARAMETERS                                              00000570
```

```
      L=1                                                    00000571
  311 CONTINUE                        -89-                   00000572
      NIT=IN*NO                                              00000580
      DO 91 I=1,NIT                                          00000590
      GRT(I)=0.                                              00000600
      GIT(I)=0.                                              00000610
      YR(I)=0.                                               0000062C
      YI(I)=0.                                               00000630
      XRT(I)=0.                                              00000640
      XIT(I)=0.                                              00000650
   91 CONTINUE                                               00000660
      TAU=2.*3.14159265358979                                00000670
      TEMP=1./FLOAT(NO)                                      0000070C
      WB=SQRT(P*P-1.0)                                       00000710
      WO2=WB*WB                                              00000720
      PB2=P*P                                                00000730
      RW=WZ**2-WB**2                                         00000740
      GAMB=GAM/8.                                            00000750
      WZ2=WZ*WZ                                              00000760
      W=WZ2                                                  00000770
      NS2=NS/2                                               00000780
      PRMT(1)=0.0                                            00000790
      PRMT(2)=TAU                                            00000800
      PRMT(3)=TAU/FLOAT(NS)                                  00000810
      PRMT(4)=1.0                                            00000820
C DECIDE WHETHER A SWEEP OR NO SWEEP                         00000840
   14 IF(NSP-1)13,13,107                                     00000850
  107 L=6                                                    00000851
      IF(L.EQ.6)GO TO 10                                     00000852
   13 CONTINUE                                               00000860
      GO TO(6,7,8,9),ISP                                     00000870
    6 CONTINUE                                               00000880
      U=0.0+0.10*(L-1)                                       00000900
      GO TO 10                                               00000910
    7 CONTINUE                                               00000920
      CPB=0.0-0.2*(L-1)                                      00000940
      GO TO 10                                               00000950
    8 CONTINUE                                               00000960
      CPL=0.0-0.10*(L-1)                                     00000980
      GO TO 10                                               00000990
    9 CONTINUE                                               00001000
      R=0.0-0.20*(L-1)                                       00001020
   10 CONTINUE                                               00001030
C TRIMMED OR UNTRIMMED                                       00001031
      CTS=CTO/SIG                                            00001032
      IF(KY-1)121,12,11                                      00001050
   11 CONTINUE                                               00001060
C   THIS IS MOMENT TRIM EQNS                                 00001070
      GNU=SQRT(0.5*SQRT(U**4+CTO**2)-U**2*0.5)               00001080
      CTSA=CTS/AA                                            00001090
      PHIH=(4./3.)*SQRT(CTO/2.)                              00001100
      PHIB=(4./3.)*GNU                                       00001110
      CTH=CTSA*6.+1./8.*PHIH                                 00001120
      THZ=(6.*CTSA+9./8.*PHIB)+U**2*(15.*CTSA+9./16.*PHIB)   00001130
      THS=-U*(16.*CTSA+1.5*PHIB)-U**3*(16.*CTSA-3./4.*PHIB)  00001140
      THC=U*GAM/PB2*(CTSA+1./48.*PHIB)-U**3*GAM/PB2*(5./9.*CTSA+1./16.  00001150
     1*PHIB)+4./3.*U*(PB2-1.)/PB2*BZ*(1.-1./2.*U*U)          00001160
      BO=GAM/PB2*(3./4.*CTSA+1./64.*PHIB)-U**2*(1./24.*CTSA+5./128.*    00001161
     1PHIB)*GAM/PB2+(PB2-1.)/PB2*BZ                          00001162
      GO TO 121                                              00001170
```

```
   12 CONTINUE                                                      00001179
C ThIS IS UNTRIMMED EQNS                     -90-                   00001180
      CB=6.*(PB2-1.)/GAM-CPB                                        00001181
      BS=U*(CB*(16.*CTS/AA+1.5*PHIB)-GAM/PB2*(CTS/AA+1./48.*PHIB))/(1.+  00001182
     1CB**2)+U**3*(-CB*(24.*CTS/AA+1.5*PHIB)+GAM/PB2*(CTS/AA+5./48.*     00001183
     2PHIB))/(1.+CB**2)-4./3.*U*(CB/(1.+CB**2))*(PB2-1.)*BZ/PB2          00001184
      BC=-U*((16.*CTS/AA+1.5*PHIB)+CB*GAM/(6.*PB2)*(6.*CTS/AA+1./8.*PHIB 00001185
     1))/(1.+CB**2)+U**3*((16.*CTS/AA+15./4.*PHIB)+CB*GAM/(6.*PB2)*(3.*  00001186
     2CTS/AA+9./16.*PHIB))/(1.+CB**2)+4./3.*U*(1./(1.+CB**2))*(1.+.5*U   00001187
     3**2)*(PB2-1.)*BZ/PB2                                              00001188
      BG=GAM/(8.*PB2)*(6.*CTS/AA+1./8.*PHIB)-GAM/(8.*PB2)*(3.*CTS/AA+    00001189
     19./16.*PHIB)*U**2+GAM/(8.*PB2)*(9./2.*CTS/AA+27./32.*PHIB)*U**4    00001190
     2+(PB2-1.)*BZ/PB2-U*GAM*CPB*BS/(48.*PB2)                           00001191
      THZ=(6.*CTS/AA+9./8.*PHIB)-(9.*CTS/AA+27./16.*PHIB)*U**2+(27./2.*  00001192
     1CTS/AA+81./32.*PHIB)*U**4-1.5*U*BS*CPB                            00001193
      THS=BS*CPB                                                       00001194
      THC=BC*CPB                                                       00001195
  121 CONTINUE                                                        00001196
      WRITE(6,100)                                                    00001197
      WRITE(6,1)                                                      00001200
      WRITE(6,601)NO,MR,NS,NH,IN,NR,ISP,NSP,KY                        00001210
      WRITE(6,2)                                                      00001220
      WRITE(6,600)P,WZ,R,RFL,RT,DPL                                   00001230
      WRITE(6,3)                                                      00001240
      WRITE(6,600)U,GAM,SD,CTO,SIG,AA                                 00001250
      WRITE(6,4)                                                      00001260
      WRITE(6,600)BZ,THS,THC,CPB,CPL,ZSC                              00001270
      WRITE(6,5)                                                      00001280
      WRITE(6,600)BG,BS,BC,THZ,PHIB,PHIH,THF                          00001290
C                                                                     00001300
C                                                                     00001310
C                                                                     00001320
C SET UP INIT CONDS AND INTEGRATE FCT TO FORM STATE AND FLOQUET        00001330
C TRAN MATRICES COLUMN BY COLUMN,THEN STORE IN OUTP                    00001340
C                                                                     00001350
C                                                                     00001360
      DO 20 KZ=1,NO                                                   00001370
      DO 15 KR=1,NO                                                   00001380
      DERY(KR)=TEMP                                                   00001390
   15 Y(KR)=0.0                                                       00001400
      Y(KZ)=1.0                                                       00001410
      CALL DHPCG(PRMT,Y,DERY,NO,IHLF,FCT,OUTP,AUX)                    00001420
      IF(IHLF-11)19,16,16                                             00001430
   16 WRITE(6,17)IHLF                                                 00001440
   17 FORMAT(5X,I10)                                                  00001450
      GO TO 999                                                       00001460
   19 CONTINUE                                                        00001470
      DO 18 NB=1,NO                                                   00001480
   18 D(NB,KZ)=PHI(NS*NO*NO+NO*(KZ-1)+NB)                             00001490
   20 CONTINUE                                                        00001500
      WRITE(6,170)                                                    00001510
  170 FORMAT(5X,1HD)                                                  00001520
      WRITE(6,160)((D(NB,KZ),KZ=1,NO),NB=1,NO)                        00001530
  160 FORMAT(4D20.7)                                                  00001540
C FIND EIGENVALUES,EIGENVECTORS,CHARACTERISTIC FUNCTIONS               00001550
      CALL DCPXRT(NO,MR,D,RSST,MAT2)                                  00001560
      WRITE(6,21)                                                     00001570
   21 FORMAT(15X,9HFREQUENCY,12X,7HDAMPING)                           00001580
      DO 23 JK=1,MR                                                   00001590
      SRT=RSST(JK,1)**2+RSST(JK,2)**2                                 00001600
```

```
      DMP=ALOG(SRT)/(2.*PRMT(2))                                   00001610
      FRQ=DATAN2(RSST(JK,2),RSST(JK,1))/PRMT(2)                    00001620
      ETA(JK)=CMPLX(DMP,FRQ)                                       00001630
      WRITE(6,22)FRQ,DMP                                           00001640
   22 FORMAT(5X,2(5X,F15.8))                                       00001650
   23 CONTINUE                                                     00001660
      WRITE(6,210)                                                 00001670
  210 FORMAT(5X,3HETA)                                             00001680
      WRITE(6,220)ETA                                              00001690
  220 FORMAT(2X,6F15.5)                                            00001700
C                                                                  00001710
C                                                                  00001720
C PULL OUT NO BY NO AND TAKE INV                                   00001730
      KK=0                                                         00001740
      DO 35 INV=1,IN                                               00001750
      DO 31 IC=1,NO                                                00001760
      DO 31 IR=1,NO                                                00001770
      KK=KK+1                                                      00001780
      DUMR(IR,IC)=REAL(AS(KK))                                     00001790
   31 DUMI(IR,IC)=AIMAG(AS(KK))                                    00001800
      CALL MINV(DUMR,DUMI,NO,DUVR,DUVI,LWL,MWM,IE)                 00001810
      KL=0                                                         00001820
      DO 32 I=1,NO                                                 00001830
      DO 32 J=1,NO                                                 00001840
      KL=KL+1                                                      00001850
      DUMRV(KL)=DUMR(J,I)                                          00001860
   32 DUMIV(KL)=DUMI(J,I)                                          00001870
C GET FT FROM FORCE                                               00001880
      CALL FORCE(NO,NS,INV,F,FM,FT)                                00001890
      WRITE(6,400)                                                 00001900
  400 FORMAT(5X,2HFT)                                              00001910
      WRITE(6,410)FT                                               00001920
  410 FORMAT(2X,4F20.7)                                            00001930
C NOW GET RHS GT                                                   00001940
      CALL DMPRD(DUMRV,FT,GTR,NO,NO,0,0,1)                         00001950
      CALL DMPRD(DUMIV,FT,GTI,NO,NO,0,0,1)                         00001960
      CALL PLAS2(GTR,1,NO,0,GRT,IN,NO,0,INV,1)                     00001970
   35 CALL PLAS2(GTI,1,NO,0,GIT,IN,NO,0,INV,1)                     00001980
      CALL DMXOUT(5,GRT,IN,NO,0,70,132,1)                          00001990
      WRITE(6,33)                                                  00002000
      CALL DMXOUT(6,GIT,IN,NO,0,70,132,1)                          00002010
      WRITE(6,34)                                                  00002020
   33 FORMAT(5X,16HREAL PART OF RHS)                               00002030
   34 FORMAT(5X,16HIMAG PART OF RHS)                               00002040
      CONTINUE                                                     00002050
C CALCULATE UNCOUP RESP YT                                         00002060
C                                                                  00002070
C FIRST CALC FOUR COEFS OF REAL AND IMAG PARTS OF GT               00002080
      KNT=0                                                        00002090
      DO 45 IV=1,NO                                                00002100
      KNS=NH*(IV-1)                                                00002110
      DO 41 IT=1,NS                                                00002120
      KNT=KNT+1                                                    00002130
      FNT(IT)=GRT(KNT)                                             00002140
   41 GNT(IT)=GIT(KNT)                                             00002150
      KNT=KNT+1                                                    00002160
      CALL DFORIT(FNT,NS,NH,AL,BL)                                 00002170
      CALL DFORIT(GNT,NS,NH,AB,BB)                                 00002180
      DO 46 ITY=1,IN                                               00002190
      SYT=0.0                                                      00002200
```

```
      PSI=6.28318/FLOAT(NS)*(ITY-1)        -92-            00002210
      AVG=CMPLX(AL(1),AB(1))/(ETA(IV))                     00002220
      DU 44 ICH=2,NH                                       00002230
      CRP=(AL(ICH)+BB(ICH))/2.                             00002240
      CIP=(AB(ICH)-BL(ICH))/2.                             00002250
      CRN=(AL(ICH)-BB(ICH))/2.                             00002260
      CIN=(AB(ICH)+BL(ICH))/2.                             00002270
      CP=CMPLX(CRP,CIP)                                    00002280
      CN=CMPLX(CRN,CIN)                                    00002290
C NOW CALC FORST YT COEFFS AND DIV                         00002300
C THEN CALC YT                                             00002310
      DUM=FLOAT(ICH-1)                                     00002320
      CDUM=CMPLX(0.0,DUM)                                  00002330
      YCP=(CDUM)-(ETA(IV))                                 00002340
      YCN=-(CDUM)-(ETA(IV))                                00002350
      CP=CP/YCP                                            00002360
      CN=CN/YCN                                            00002370
      QCT=QP+QN                                            00002380
      QST=QP-QN                                            00002390
      GFT(ICH)=QCT*COS(FLOAT(ICH-1)*PSI)+CST*SIN(FLOAT(ICH-1)*PSI)*(0.0,00002400
     11.0)                                                 00002410
   44 SYT=SYT+GFT(ICH)                                     00002420
      YTR(ITY)=REAL(SYT)-REAL(AVG)                         00002430
   46 YTI(ITY)=AIMAG(SYT)-AIMAG(AVG)                       00002440
      CALL PLAS2(YTR,IN,1,0,YR,IN,NO,0,1,IV)               00002450
   45 CALL PLAS2(YTI,IN,1,0,YI,IN,NO,0,1,IV)               00002460
      CALL DMXOUT(7,YR,IN,NO,0,70,132,1)                   00002470
      WRITE(6,47)                                          00002480
   47 FORMAT(5X,15HREAL PART OF YT)                        00002490
      CALL DMXOUT(8,YI,IN,NO,0,70,132,1)                   00002500
      WRITE(6,48)                                          00002510
   48 FORMAT(5X,15HIMAG PART OF YT)                        00002520
C    FOUR ANALZ YT                                         00002530
      KRT=0                                                00002540
      DO 71 I=1,NO                                         00002550
      KRS=NH*(I-1)                                         00002560
      DO 72 J=1,NS                                         00002570
      KRT=KRT+1                                            00002580
   72 FYR(J)=YR(KRT)                                       00002590
      KRT=KRT+1                                            00002600
      CALL DFORIT(FYR,NS,NH,A,B)                           00002610
      DO 73 K=1,NH                                         00002620
   73 YRFA(KRS+K)=A(K)**2+B(K)**2                          00002630
      DO 74 K=1,NH                                         00002640
   74 YRFA(KRS+K)=SQRT(YRFA(KRS+K))                        00002650
   71 CONTINUE                                             00002660
      CALL DMXOUT(17,YRFA,NH,NO,0,60,132,1)                00002670
      WRITE(6,703)                                         00002680
  703 FORMAT(5X,15HHARMONICS OF YR)                        00002690
      KIT=0                                                00002700
      DO 81 I=1,NO                                         00002710
      KIS=NH*(I-1)                                         00002720
      DO 82 J=1,NS                                         00002730
      KIT=KIT+1                                            00002740
   82 FYI(J)=YI(KIT)                                       00002750
      KIT=KIT+1                                            00002760
      CALL DFORIT(FYI,NS,NH,A,B)                           00002770
      DO 83 K=1,NH                                         00002780
   83 YIFA(KIS+K)=A(K)**2+B(K)**2                          00002790
      DO 84 K=1,NH                                         00002800
```

```
   84 YIFA(KIS+K)=SQRT(YIFA(KIS+K))        -93-              00002810
   81 CONTINUE                                               0C002820
      CALL DMXOUT(16,YIFA,NH,NO,0,60,132,1)                  00002830
      WRITE(6,803)                                           00002840
  803 FORMAT(5X,15HHARMONICS OF YI)                          00002850
C NEED TO STORE YR AND YI IN YT AS NO BY IN                 00002860
C                                                            00002870
C                                                            00002880
      DO 49 IT=1,IN                                          00002890
      DO 49 IG=1,NO                                          00002900
      KM=IN*(IG-1)+IT                                        000C2910
      MSTOR=NO*(IT-1)+IG                                     00002920
   49 YT(MSTOR)=CMPLX(YR(KM),YI(KM))                         000C2930
C NOW CALC STATE RESP XT                                    00002940
C                                                            0C002950
C NEED TO PULL OUT NO BY NO A(T) AND MPY BY NO BY 1 Y(T)    00002960
      LL=0                                                   00002970
      JJ=0                                                   000C2980
      DO 55 ITL=1,IN                                         00002990
      LK=0                                                   00003000
      DO 51 IC=1,NO                                          00003010
      DO 51 IR=1,NO                                          00003020
      LL=LL+1                                                00003030
      LK=LK+1                                                00003040
   51 DUMA(LK)=AS(LL)                                        00003050
      MM=0                                                   00003060
      DO 52 JR=1,NO                                          00003070
      JJ=JJ+1                                                00003080
      MM=MM+1                                                00003090
   52 DUMY(MM)=YT(JJ)                                        0C003100
      CALL DMP2C(DUMA,DUMY,XT,NO,NO,0,0,1)                   00003110
      DO 53 JK=1,NO                                          00003120
      XTR(JK)=REAL(XT(JK))                                   00003130
   53 XTI(JK)=AIMAG(XT(JK))                                  00003140
      CALL PLAS2(XTR,1,NO,0,XRT,IN,NO,0,ITL,1)               00003200
   55 CALL PLAS2(XTI,1,NO,0,XIT,IN,NO,0,ITL,1)               0C003210
      CALL DMXOUT(9,XRT,IN,NO,0,70,132,1)                    00003220
      WRITE(6,56)                                            00003230
   56 FORMAT(5X,12HREAL PART XT)                             00003240
      KNT=0                                                  00003250
      DO 61 IV=1,NO                                          0CC03260
      KNS=NH*(IV-1)                                          00003270
      DO 62 IT=1,NS                                          00003280
      KNT=KNT+1                                              00003290
   62 FXT(IT)=XRT(KNT)                                       0000330C
      KNT=KNT+1                                              0CC03310
      CALL UFORIT(FXT,NS,NH,A,B)                             00003320
      DO 63 ISTR=1,NH                                        00003330
   63 XFA(KNS+ISTR)=A(ISTR)**2+B(ISTR)**2                    00C03340
      DO 64 ISTR=1,NH                                        00003350
   64 XFA(KNS+ISTR)=SQRT(XFA(KNS+ISTR))                      00003360
   61 CONTINUE                                               00003370
      CALL DMXOUT(14,XFA,NH,NO,0,60,132,1)                   0000338C
      WRITE(6,603)                                           0C003390
  603 FORMAT(5X,16HHARMONICS OF XRT)                         00003400
      CALL DMXOUT(10,XIT,IN,NO,0,70,132,1)                   000C3410
      WRITE(6,57)                                            00003420
   57 FORMAT(5X,12HIMAG PART XT)                             0C003430
      CONTINUE                                               000C3440
C NEED TO CONVERT XT TO VIB SHRS AND MOMS                   00003450
```

```
C FOUR ANALYZE SHRS AND MOMS TO OBTAIN HARM COMPS                    00003460
C                                                                    00003470
      CALL BSHR(XRT,FM,RBSHR)                                        00003480
      CALL ZSHR(XRT,FM,RBSHR,RZSHR)                                  00003490
      CALL RSHR(XRT,RBSHR,RZSHR)                                     00003500
      DO 93 ITB=1,IN                                                 00003501
      PSI=6.2831853/FLOAT(NS)*(ITB-1)                                00003502
      BBAR=B0+BS*SIN(PSI)+BC*COS(PSI)                                00003503
      BBD=BS*COS(PSI)-BC*SIN(PSI)                                    00003504
      XRT(ITB)=XRT(ITB)+BBAR                                         00003505
   93 XRT(ITB+65)=XRT(ITB+65)+BBD                                    00003506
      CALL DMXOUT(15,XRT,IN,NO,0,70,132,1)                           00003508
      WRITE(6,94)                                                    00003509
   94 FORMAT(5X,14HREAL XT W/B BD)                                   00003510
      KNT=0                                                          00003511
      DO 99 IV=1,NO                                                  00003512
      KNS=NH*(IV-1)                                                  00003513
      DO 95 IT=1,NS                                                  00003514
      KNT=KNT+1                                                      00003515
   95 FXBT(IT)=XRT(KNT)                                              00003516
      KNT=KNT+1                                                      00003517
      CALL DFORIT(FXBT,NS,NH,A,B)                                    00003518
      DO 96 ISTR=1,NH                                                00003519
   96 XFBA(KNS+ISTR)=A(ISTR)**2+B(ISTR)**2                           00003520
      DO 97 ISTR=1,NH                                                00003521
   97 XFBA(KNS+ISTR)=SQRT(XFBA(KNS+ISTR))                            00003522
   99 CONTINUE                                                       00003523
      CALL DMXOUT(16,XFBA,NH,NO,0,60,132,1)                          00003524
      WRITE(6,990)                                                   00003525
  990 FORMAT(5X,16HHARMONICS OF XBT)                                 00003526
      CALL BMOM(XRT)                                                 00003527
      CALL ZMOM(XRT)                                                 00003528
      WRITE(6,300)                                                   00003529
  300 FORMAT(5X,4HR,RW)                                              00003530
      WRITE(6,310)R,RW                                               00003531
  310 FORMAT(2X,2F20.7)                                              00003532
      L=L+1                                                          00003533
      IF(L.LT.7)GO TO 311                                            00003534
  999 CONTINUE                                                       00003535
 1000 CONTINUE                                                       00003540
      STOP                                                           00003550
      END                                                            00003560
```

9.3.2 Subroutine Listings

No.	Name	Description	Source
1	BMOM	Computes rotating system flap moments and fixed system pitch and roll moments	Part of research
2	BSHR	Computes rotating system flap shears and fixed system vertical shears	Part of research
3	DDET5	Computes a vector of derivative values given a vector of function values	IBM Scientific Subroutine Package (SSP)
4	DFORIT	Produces the Fourier coefficients of a tabulated **function**	IBM SSP
5	DHPCG	Solves a system of first order ordinary general differential equations with given initial values using Hamming's modified predictor-corrector method	IBM SSP
6	DMPRD	Multiplies two matrices to form a resultant matrix	IBM SSP
7	DMP2Q	Multiplies two complex matrices to form a complex resultant matrix	Part of research Modified DMPRD
8	DMXOUT	Produces an output listing of any sized array on logical unit 6	IBM SSP
9	FCT	Used with DHPCG it computes the right hand sides DERY of the system to given values of X and Y	Part of research
10	FORCE	Computes the forcing functions on the right hand side of the flap-lag equations	Part of research
11	LOC	Used to reference elements within a matrix stored in a vector fashion	IBM SSP

No.	Name	Description	Source
12	MAT 2	Used with OCPXRT it computes the eigenfunctions given the eigenvalues and eigenvectors	Wilkinson, J. H. The Algebraic Eigenvalue Problem Part of research
13	MINV	Inverts a complex matrix	Part of research Modified MINV of IBM SSP
14	MTXMUL	Used with OCPXRT it multiplies matrices	Wilkinson, J. H. The Algebraic Eigenvalue Problem
15	OCPXRT	Extracts eigenvalues from Floquet Transition Matrix and calculates eigenvectors	Wilkinson, J. H. The Algebraic Eigenvalue Problem
16	OUTP	Used with DHPCG it handles the output	IBM SSP Part of research
17	OVUN	Used with MINV to avoid possible overflow conditons	IMB SSP Part of research
18	PLAS 2	Places elements from an array into another array format	Part of research
19	RSHR	Computes the radial shears in the rotating system	Part of research
20	SERCH	Used with OCPXRT it searches for the largest eigenvalues	Wilkinson, J. H. The Algebraic Eigenvalue Problem
21	TRACE	Used with OCPXRT it computes the trace of a matrix	Wilkinson, J. H. The Algebraic Eigenvalue Problem
22	ZMOM	Computes rotating system lag moments	Part of research
23	ZSHR	Computes rotating system lag shears and fixed system lateral and longitudinal shears	Part of research